ANNUAL REVIEWS

Annual Review of Plant Biology

Regulation and Evolution of C_4 Photosynthesis

Urte Schlüter and Andreas P.M. Weber

Institute of Plant Biochemistry, Cluster of Excellence on Plant Sciences (CEPLAS), Heinrich Heine University, 40225 Düsseldorf, Germany; email: u.schlueter@hhu.de, andreas.weber@hhu.de

Annu. Rev. Plant Biol. 2020. 71:183–215

First published as a Review in Advance on March 4, 2020

The *Annual Review of Plant Biology* is online at plant.annualreviews.org

https://doi.org/10.1146/annurev-arplant-042916-040915

Keywords

CO_2 fixation, evolution, redox regulation, transcriptional regulation, posttranslational regulation

Abstract

C_4 photosynthesis evolved multiple times independently from ancestral C_3 photosynthesis in a broad range of flowering land plant families and in both monocots and dicots. The evolution of C_4 photosynthesis entails the recruitment of enzyme activities that are not involved in photosynthetic carbon fixation in C_3 plants to photosynthesis. This requires a different regulation of gene expression as well as a different regulation of enzyme activities in comparison to the C_3 context. Further, C_4 photosynthesis relies on a distinct leaf anatomy that differs from that of C_3, requiring a differential regulation of leaf development in C_4. We summarize recent progress in the understanding of C_4-specific features in evolution and metabolic regulation in the context of C_4 photosynthesis.

Contents

1. INTRODUCTION

The evolution of oxygenic photosynthesis fundamentally changed the geosphere and biosphere and also the energy transformations that support life on Earth (60). In oxygenic photosynthesis, the energy contained in sunlight is harvested and used for the extraction of electrons from water and for the buildup of a proton gradient, eventually leading to the production of adenosine triphosphate (ATP) and nicotinamide adenine dinucleotide phosphate hydrogen (NADPH). These energy and reducing equivalents are then used for the reduction of CO_2 into carbohydrates in the Calvin-Benson cycle. The process of CO_2 fixation is catalyzed by ribulose 1,5 bisphosphate carboxylase/oxygenase (Rubisco), which can react either with CO_2, forming two molecules of 3-phosphoglycerate (3PGA), or with O_2, forming one molecule of 3PGA and one molecule of 2-phosphoglycerate (2PG). 3PGA can directly reenter the Calvin-Benson cycle. However, 2PG inhibits at least three enzymes of the Calvin-Benson cycle: triose phosphate isomerase, sedoheptulose 1,7-bisphosphatase (SBP), and phosphofructokinase (62). It therefore must be removed quickly. At least three different metabolic routes for the removal of 2PG have evolved in cyanobacteria, and in all vascular plants 2PG is metabolized by the photorespiratory pathway, which converts two molecules of 2PG into 3PGA, CO_2, and NH_3 (54). During the early stages of evolution of oxygenic photosynthesis, the atmosphere of Earth contained very little oxygen and large amounts of CO_2. Hence the gas composition of the atmosphere favored the carboxylase reaction of Rubisco, and the oxygenase reaction played only a very minor metabolic role for photosynthetic organisms. However, over billions of years of oxygenic photosynthesis, the oxygen levels rose and the CO_2 concentration declined. During the Eocene-Oligocene transition, the atmospheric CO_2 concentrations decreased to 450 ppm or less (206). Under these atmospheric conditions, many C_3 plants frequently experience carbon limitation, excess light energy is unproductively dissipated by various protection mechanisms, and photorespiration represents a major highway of carbohydrate metabolism (75). In a typical C_3 plant, the majority of NH_3 released during photorespiration is refixed at the expense of ATP and reducing power. Also, the CO_2 that is released by photorespiration can be refixed by Rubisco, or it gets lost back into the atmosphere. Losses of CO_2 and energy by photorespiration are particularly serious when the capacity for O_2 binding of Rubisco increases.

Fossil evidence indicates that during the Oligocene, the first plant lineages evolved a carbon concentration mechanism that is able to reduce the rate of photorespiration [see Hennacy & Jonikas (79) for a discussion of algal and cyanobacterial types of carbon concentrating mechanisms]. In these plants, CO_2 is prefixed as HCO_3^- by an enzyme that displays no oxygenase activity, phospho*enol*pyruvate carboxylase (PEPC), forming the C_4 acid oxaloacetate (OAA) as the first detectable reaction product. CO_2 is released again from C_4 metabolites at the site of Rubisco, thereby forming a high CO_2 atmosphere around the enzyme. In crassulacean acid metabolism (CAM), the prefixation of CO_2 by PEPC is temporally separated from the Rubisco reaction. Prefixation takes place primarily at night when transpiratory water loss is low, and the C_4 reaction products are stored in the vacuole, mainly in the form of malate. During the day malate is decarboxylated, creating a high CO_2 atmosphere around Rubisco while the stomata remain closed. CAM plants are therefore characterized by remarkably high water-use efficiency. In C_4 species, the PEPC and Rubisco reactions are separated spatially. CO_2 is prefixed in one leaf compartment by PEPC and transported to the Rubisco-containing compartment in the form of a C_4 metabolite, thus producing a high CO_2 atmosphere around Rubisco (**Figure 1**). This arrangement represses the oxygenase reaction and allows Rubisco to operate near substrate saturation at high light conditions (110). Implementation of the C_4 pathway underpinned the evolution of highly productive plant species with improved light conversion as well as water- and nitrogen-use efficiency. The C_4 pathways evolved independently in more than 60 plant species from different phylogenetic groups, among them crop plants such as maize, sugarcane, sorghum, millet, teff, and amaranth (154).

Before the discovery of their underlying biochemistry, C_4 species had already been distinguished by high vein density and the typical Kranz anatomy in the cross sections of their leaves (57, 74). Two different cell types are arranged concentrically around the leaf veins: an internal ring consisting of large enforced bundle sheath cells (Kranz) and a second external layer of mesophyll cells. Later studies established that both cell types represent different compartments of the C_4 carbon concentration mechanism. The first CO_2 fixation step by the PEPC takes place in the outer mesophyll cell tissue, while the Rubisco reaction is confined to the bundle sheath. A high bundle sheath-to-mesophyll cell ratio ensures the efficient exchange of metabolites between the two cell types. The increased metabolic role of the bundle sheath in the carbon fixation process in the C_4 leaves is reflected by an increase in the number and arrangement of organelles in this cell type. The enforced cell walls of the bundle sheath cells minimize the leakage of CO_2 from the Rubisco-containing cells. Although Kranz anatomy is characteristic for the majority of and most efficient C_4 species, C_4 photosynthesis has more recently also been found in succulent plants with bands of mesophyll and bundle sheath tissue around a water body (64, 163) or even a single cell that contains dimorphic plastids (186).

The basic biochemical principle of the CO_2 pump is similar in all C_4 species. CO_2 entering the mesophyll cells is converted into bicarbonate by carbonic anhydrases (CAs) and then reacts with PEPC, forming the C_4 organic acid OAA. OAA is next converted to malate and/or aspartate. Malate and/or aspartate then diffuses through plasmodesmata to the bundle sheath cells. There, decarboxylation of the C_4 acid generates an elevated CO_2 atmosphere so that the oxygenase reaction of the Rubisco is strongly reduced. The C_4 cycle is completed by the regeneration of phosphoenolpyruvate (PEP) as a substrate for PEPC by pyruvate orthophosphate dikinase (PPDK), a recycling step incurring additional energy costs.

Beside this common basic C_4 setup, the various C_4 lineages evolved distinct solutions for many C_4 functions and adjustment steps (133). This is particularly apparent for the decarboxylation step in bundle sheath cells that can be realized by three different enzymatic functions: the plastidial NADP-malic enzyme (NADP-ME) (**Figure 1*a***), the mitochondrial NAD malic enzyme (NAD-ME) (**Figure 1*b***), the cytosolic PEP carboxykinase (PEPCK), or a combination of these enzymes

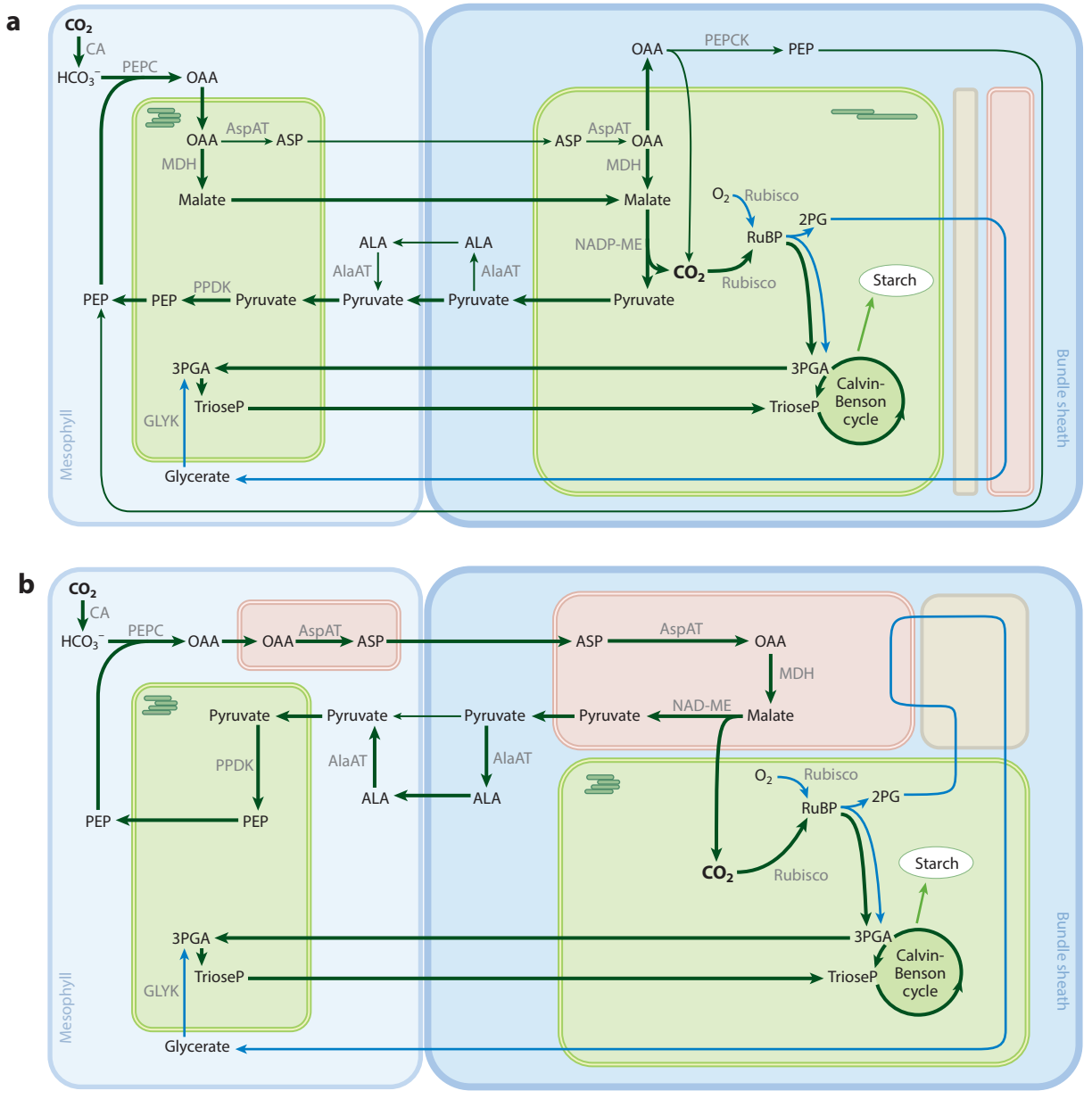

(*Caption appears on following page*)

Figure 1 (*Figure appears on preceding page*)

Model of the C_4 metabolism in (*a*) a NADP-ME species (*Zea mays*) and (*b*) a NAD-ME species (*Gynandropsis gynandra*). (*a*) Model represents NADP-ME as the main decarboxylating enzymes and malate/pyruvate as the main acid exchange, but it is supplemented by the activity of PEPCK in the bundle sheath and additional exchange of aspartate and alanine between mesophyll and the bundle sheath. The reduction steps of the Calvin-Benson cycle take place in the mesophyll and require additional transport of 3PGA and trioseP between the two cell types. The GLYK step of photorespiration also takes place in the mesophyll cell. (*b*) Model represents C_4 photosynthesis in *G. gynandra* with NAD-ME as the main decarboxylating enzyme and aspartate/alanine as the main acid exchange. In contrast to other NAD-ME species, both cell types show high abundance of mitochondrial AspAT. Enzymes are shown in gray text. Abbreviations: 3PGA, 3-phosphoglycerate; ALA, alanine; AlaAT, alanine aminotransferase; ASP, aspartate; AspAT, aspartate aminotransferase; CA, carbonic anhydrase; GLYK, glycerate kinase; MDH, malate dehydrogenase; NAD-ME, nicotinamide adenine dinucleotide malic enzyme; NADP-ME, nicotinamide adenine dinucleotide phosphate malic enzyme; OAA, oxalacetate; PEP, phosphoenolpyruvate; PEPC, phosphoenolpyruvate carboxylase; PEPCK, PEP carboxykinase; PPDK, pyruvate orthophosphate dikinase; Rubisco, ribulose 1,5-bisphosphate carboxylase/oxygenase; RuBP, ribulose 1,5 bisphosphate.

(25, 66, 141). Besides the cell-specific upregulation of the C_4 core enzymes, the integration of the C_4 cycle into the biochemistry of the leaf also requires changes in the abundance of specific transporters and the regulation and kinetics of connected pathways. In NADP-ME species, malate transports not only carbon but also reductive power from the mesophyll to the bundle sheath cells, and this has consequences for the differential setup of the energy-providing photosystems in these cells. Rubisco as the starting point for the Calvin-Benson cycle and photorespiratory cycle is active only in the bundle sheath, and all other enzymes of these pathways must adjust to the two-cell situation in the C_4 leaf (**Figure 1**). Further down, sucrose and starch metabolism as well as nitrogen assimilation would also be affected (24). In many C_4 species, the mesophyll bears the larger part of the light reaction and the production of ATP and reducing equivalents. This has consequences for the redox balances between the two different cell types and the distribution of reactions between the two cell types, especially the ones needing a low reduction potential (178). The differences between the light-related activities of the mesophyll and bundle sheath cells are particularly apparent in NADP-ME species, where chloroplasts of the mesophyll and bundle sheath cells show distinct ratios of the photosystems and chloroplast ultrastructure (chloroplast dimorphism).

The requirements for the regulation of the members of the pathways listed above and the currently known mechanisms are described in the following paragraphs in more detail. The regulation of cell specificity and abundance of the main players of the C_4 core have been investigated quite extensively and have revealed control operating on epigenetic, transcriptional, posttranscriptional, translational, posttranslational, and protein-activity levels (**Table 1**) (147). Many C_4 regulatory mechanisms are shared between members of different pathways and revert to regulatory mechanisms also operating in C_3 plants (28). Genes encoding C_4 core enzymes have, for instance, gained light- and plastid-regulated elements, allowing coordination of the C_4 cycle with the connected pathways, such as the Calvin-Benson cycle. Under fluctuating environmental conditions, the efficiency of C_4 photosynthesis will also depend on the coordination of energy balance between the mesophyll and bundle sheath localized reactions (16).

2. EVOLUTION OF C_4 PHOTOSYNTHESIS

All currently known elements required for the C_4 pathway have also been found in their ancestral C_3 relatives, and this might be one of the reasons why the C_4 cycle could evolve so many times and in such distant plant groups as, for instance, the grasses, the Asteraceae, and the Cleomaceae (155). However, the multiple cases of parallel but independent evolution are also surprising since the evolution of C_4 entails complex changes to the whole leaf biochemistry and architecture. In some branches of the plant kingdom, such as the Brassicaceae and the monocot clade containing the Bambusoideae, Ehrhartoideae, and Pooideae (BEP), C_4 species are absent (155). The evolution

Table 1 Regulatory mechanism involved in different aspects of C_4

Process	Target of regulation	Species	Type	Description	Reference(s)
Anatomy	BS cell activation/ Vein spacing	*Zea mays*	*Trans*	TF (e.g., SCR/SHR, DOT5, G2/GLK)	168, 176, 192, 193
		Echinochloa glabrescens	*Trans*	TF	40
		Flaveria	*Trans*	TF (e.g., ATHB8-like, SCR-like, ARF3, IAA7)	71, 101
		Gynandropsis gynandra	*Trans*	TF	12, 99
	Cell cycle/division/size	*Flaveria*	*Trans*	TF (e.g., DWARF4)	101
		G. gynandra	*Trans*	TF	99
		Panicum virgatum	*Trans*	TF (MYB59)	144
	Plastid development	*Z. mays*	*Trans*	TF (e.g., G2, GLK)	104, 176, 192
		Flaveria	*Trans*	TF	101
		Setaria viridis	*Trans*	TF (e.g., GLK, IDD5, SMAD/FHA, SIG2/3, pTAC12)	86
	BS wall formation	*P. virgatum*	*Trans*	TF (e.g., MYB4)	144
		Z. mays	*Trans*	TF	190
	Photosystem formation	*Z. mays*	*Trans*	TF	190
		Z. mays	Posttranscriptional	HFC136	39
C_4 shuttle	CA	Multiple grasses	Histone	Histone modification (e.g., mesophyll- and BS-specific code)	78, 140
		G. gynandra	*Cis*	Cell specificity (e.g., MEM element in UTR)	87, 197
		Flaveria	*Cis*	Cell specificity (e.g., promoter element)	175
		Neurachne munroi	*Cis*	Loss of targeting signal	38
	PEPC	*Z. mays*	Histone	Histone modification (e.g., mesophyll- and BS-specific methylation)	43, 105
		Z. mays	*Cis*	Promoter elements	90, 174, 190
		Flaveria	*Cis*	Cell specificity (e.g., mesophyll-enhancing module MEM1)	72
		Z. mays, *Flaveria*	*Trans*	Interaction with promoter elements (e.g., DOF1, DOF2)	89, 196, 200
		Z. mays	*Trans*	Antagonistical binding of bHLH TFs to promoter	69
		Z. mays	Posttranslational, Kinetic	BS-specific protein turnover	3
		Flaveria	Kinetic	Phosphorylation	4

(*Continued*)

Table 1 (*Continued*)

Process	Target of regulation	Species	Type	Description	Reference(s)
	NADP-ME	*Z. mays*	*Cis*	Transcript abundance (e.g., UTR elements)	134
		Flaveria	*Cis*	Cell specificity (e.g., BS elements in UTRs, promoter)	5, 102, 116
		Z. mays	*Cis*	Catalytic efficiency, pH regulation, oligomerization	7
		Z. mays	*Trans*	Synergistical binding of bHLH TFs to promoter	21
	NAD-ME	*G. gynandra*	*Cis*	Cell specificity (e.g., in coding sequence)	26
	PPDK	*Z. mays*	Histone	Histone modification	46
		Z. mays	*Cis*	Cell specificity, light regulation	119, 135, 190
		Flaveria	*Cis*	Cell specificity (e.g., promoter element)	150
		G. gynandra	*Cis*	Cell specificity (e.g., UTR elements)	87, 197
		Z. mays	Posttranslational	Cell specificity (e.g., regulatory protein)	65
		G. gynandra	Posttranscriptional	mRNA accumulation	58
		Z. mays	Kinetic	Phosphorylation	31, 32
	PCK	Multiple species	Kinetic	Phosphorylation	107, 167
	Multiple targets	*G. gynandra*	*Cis*	Cell-specific elements (duons) in UTR and exon	148
		G. gynandra	*Trans*	Recruitment plastid and light regulatory network	28
		Multiple grasses	Histone	Histone modification (e.g., mesophyll- and BS-specific code)	80, 140
CBC	RbcLSU	*Z. mays*	Posttranscriptional	BS-specific binding of RLSB protein	22, 203
		Z. mays	*Trans*	Cell specificity, light regulation	120
		Z. mays	Posttranslational	Cell specificity (e.g., cell-specific degradation, stabilization)	27
		S. viridis	Posttranscriptional	RNA stabilization	86

(*Continued*)

Table 1 (*Continued*)

Process	Target of regulation	Species	Type	Description	Reference(s)
	RbcSSU	*Z. mays*	*Cis*	Cell specificity (e.g., cell and light regulatory elements)	201
		Z. mays	*Trans*	Cell specificity (e.g., TRM1 repressor in mesophyll), light regulation	14, 143, 158, 183, 201
		Amaranthus edulis, *Flaveria*	*Cis*	UTR elements	137, 138
	Multiple targets	*G. gynandra*	Posttranscriptional	mRNA accumulation	58
		P. virgatum, *S. viridis*	*Trans*	Regulation by CP12	86, 144
PR	GDCP	*Flaveria*	*Cis*	Cell specificity (BS element in promoter)	162
		Flaveria	Posttranscriptional	RNA decay	199

Abbreviations: ARF, ADP-ribosylation factor; bHLH, basic helix-loop-helix; BS, bundle sheath; CA, carbonic anhydrase; CBC, Calvin-Benson cycle; DOF, DNA binding with One Finger; GDCP, glycine decarboxylase system P-protein; IAA, indole-3-acetic acid; IDD, INDETERMINATE DOMAIN; MEM, mesophyll-enhancing molecule; mRNA, messenger RNA; NAD-ME, nicotinamide adenine dinucleotide malic enzyme; NADP-ME, nicotinamide adenine dinucleotide phosphate malic enzyme; PEPC, phosphoenolpyruvate carboxylase; PPDK, pyruvate orthophosphate dikinase; PR, photorespiratory pathway; pTAC, tac-promoter; RbcSSU, Rubisco small subunit; SCR-like, SCARECROW-like; SCR/SHR, SCARECROW/SHORT ROOT; TF, transcription factor; TRM, tissue resident memory T; UTR, untranslated region.

of the C_4 cycle is therefore dependent on the co-occurrence of external factors such as favorable climate conditions as well as internal factors such as genetic, architectural, and biochemical preconditions.

The repression of the photorespiratory oxygenase reaction in C_4 plants is particularly advantageous under high light and temperature but low CO_2 conditions (16). The drop in atmospheric CO_2 pressure starting around 30 Mya is therefore thought to represent an important ecological driver for the evolution of C_4 photosynthesis (53). More recent modeling approaches showed, however, that even under higher CO_2 concentration, arid conditions causing the closure of stomata could have promoted C_4 evolution (207). Under these conditions, nitrogen availability and allocation within the plant could have contributed to the evolution and expansion of C_4 plants (19, 207). After the establishment of the C_4 pathway, C_4 grasses were also able to adapt to colder climate zones and new ecological niches (194).

The absence of C_4 species from wide parts of the plant kingdom, however, indicates that internal preconditions are also essential for the evolution of C_4 photosynthesis. So far, primarily architectural limitations concerning the site and metabolic potential of the bundle sheath cells have been identified as limiting factors (34). For species with advantageous anatomical preconditions, the implementation of a basic C_4 cycle could possibly be achieved by a few changes in the abundance and cell specificity of the core C_4 enzymes (113). The species *Alloteropsis semialata*, for instance, includes very closely related congeners with C_3, C_3-C_4 intermediates, and C_4 photosynthesis (112). However, for an efficient C_4 shuttle in a highly productive leaf, numerous small adjustments of whole leaf metabolism are necessary (77, 133, 153, 198).

The complex trait of C_4 photosynthesis evolved not in a single step but via intermediate stages (77, 112, 153, 198). Beyond anatomical changes, such as the amplification of organelle numbers

and their positioning in bundle sheath cells, a key initial step involves a pronounced change in the distribution pattern of the glycine decarboxylating reaction in the photorespiratory pathway, from ubiquitous toward exclusive localization in the bundle sheath (125, 145, 146). The absence of a functional glycine decarboxylase system in the mesophyll would lead to an accumulation of photorespiratory glycine and the formation of a concentration gradient from mesophyll to bundle sheath, which drives transport of glycine to the bundle sheath. There, the enhanced activity of the decarboxylation step would generate an increased CO_2 concentration around the bundle sheath Rubisco (125). Plant species displaying such a glycine pump have been found in close phylogenetic proximity to C_4 species in the genera *Flaveria* (121), *Heliotropium* (128, 184), *Neurachne* (37), *Alloteropsis* (112), *Homolepis* (92), *Anticharis* (91), *Blepharis* (61), and *Salsoleae* (163, 187), but also in groups without any C_4 relatives (e.g., *Moricandia*, *Diplotaxis*) (155). Species with an active glycine pump are often termed as C_3-C_4 intermediates or C_2 photosynthesis species. Gas exchange measurements showed that the limited CO_2 concentrating effect generated by glycine decarboxylation in the bundle sheath results in a decreased CO_2 compensation point, which is below typical values for C_3 but above that of C_4 species in these intermediates (160, 184). Furthermore, these intermediates were also characterized by increased organelle numbers and changes in the organization of the bundle sheath organelles.

A complete relocation of the glycine decarboxylase reaction to the bundle sheath cells requires additional adjustments within the metabolic network of the leaf. In the glycine decarboxylase reaction, two molecules of glycine are converted into one molecule each of serine, CO_2, NH_3, and NADH. Transport of photorespiratory glycine from the mesophyll to the bundle sheath will therefore transport not only net carbon, but also nitrogen and reducing equivalents. Balancing of the nitrogen metabolism between the two cell types will require back transport of nitrogen-containing metabolites. Computational modeling of C_3-C_4 intermediate metabolism identified shuttles of glutamate/OAA, alanine/pyruvate, and aspartate/malate, as well as the associated enzyme activities as the most likely candidates for the mediation of nitrogen balance between the mesophyll and bundle sheath in these intermediate species (115). The predicted increases in the transport of these metabolites would therefore put pressure on reactions that are also involved in the C_4 pathways. Hence, the evolution of a glycine pump would push the metabolism between the mesophyll and bundle sheath toward a C_4-like metabolite exchange. Any increase in the decarboxylation reaction in the bundle sheath and of PEPC activity in the mesophyll would enhance the metabolite exchange, and in the end the increase and optimization of the flux through this cycle would result in a C_4 pump (115). Thus, the evolution of the glycine pump opens the path toward the evolution of a bona fide C_4 cycle (50, 115). The existence of species with an active glycine pump but without any C_4 relatives (e.g., *Moricandia*, *Mollugo*), however, indicates that the intermediate stages can be stable evolutionary end points in their own right (35).

The evolution of a complete C_4 shuttle, even at a basic level, requires changes in the abundance and cell specificity of multiple genes. Most of the core C_4 enzymes are encoded by multigene families (11), but the expression patterns of the gene copies available in the different C_3 ancestral species could vary greatly, thus facilitating or constraining C_4 evolution (127). In monocot species, preferences for specific gene lineages of several C_4 enzymes could be observed, indicating their particular suitability for C_4 photosynthesis (33). Gene lineages co-opted into C_4 usually show already high expression levels in the C_3 ancestors (127). Gene duplication could have enabled the C_4-favorable changes in some enzymes (7, 21, 55). The absence of a particular gene lineage in the C_3 background could, however, demand additional adjustments or alternative solutions for the fulfilment of a specific C_4 function (159). A recent analysis of the grass family showed that genes with new attributes could also be acquired by lateral gene transfer. In *A. semialata*, a C_4-optimized PEPCK was acquired by a horizontal gene transfer from a distantly related C_4 grass (49).

After the installation of the core C_4 shuttle, efficient C_4 photosynthesis also depends on multiple adjustment steps in the C_4 leaf metabolism (77). The importance of numerous optimizations within the C_4 pathway is supported by the identification of multiple regulatory mechanisms on many different levels of the C_4 core shuttle and related pathways in advanced C_4 species (133) (see Section 3). A large-scale genome-wide scan for positive selection identified 88 sites connected to the evolution of C_4 photosynthesis in *Zea mays*, *Sorghum bicolor*, and *Setaria italica*. Besides C_4 shuttle enzymes and transporters, positive selection sites were also found in genes of the Calvin-Benson cycle and photorespiratory pathway (82)—two pathways that are split between the mesophyll and bundle sheath cells in C_4 species. Additionally, new C_4 candidate genes connected, for instance, to architectural features could be identified (82). Changes in the expression patterns of C_4 genes could also often be connected to the recruitment of *cis* elements that are already present in the C_3 background (28, 149). The timing in evolution of these C_4 development and optimization steps can thereby vary between the different lineages (198). Further support for the smooth transition from C_3 to C_4 comes from computational modeling (77), which described a Mount Fuji landscape consisting of numerous adjustments that could be fixed due to their contribution to plant fitness. Accumulation of C_4-favorable mutations in a population could also allow for larger fitness gains via hybridization.

3. CHANGES TO THE REGULATION OF METABOLIC PATHWAYS DURING C_4 EVOLUTIONS

3.1. Photorespiration in Intermediates and C_4

Relocation of the photorespiratory glycine decarboxylase activity exclusively to bundle sheath cells establishes the glycine-based CO_2 pump in C_3-C_4 intermediates and represents a key step in the evolutionary path from C_3 to C_4 photosynthesis. Bundle sheath-specific localization of the P protein of the glycine decarboxylase system has been found in all C_3-C_4 intermediates investigated so far, including *Moricandia arvensis*, *Moricandia nitens*, *Moricandia sinaica*, *Moricandia suffruticosa*, *Panicum milioides*, *Flaveria floridana*, *Flaveria linearis*, *Mollugo verticillata* (84), *Diplotaxis tenuifolia* (180), *Brassica gravinae* (179), *Euphorbia acuta* (157), *Portulaca cryptopetala* (188), *Heliotropium convolvulaceum*, *Heliotropium greggii* (128), *Homolepis aturensis*, *Steinchisma hians*, and *Neurachne minor* (92). The mechanisms underpinning this decisive change in the expression pattern of a metabolic enzyme are therefore particularly interesting and have been studied in more detail in the genera *Moricandia* (2) and *Flaveria* (162).

In *Flaveria*, the C_3 ancestors possess two copies of the glycine decarboxylase P (GLDP) protein-encoding gene; one is ubiquitously expressed in the leaf tissue (*GLDPB*) and the other one exclusively in the bundle sheath (*GLDPA*) (162). A gradual decrease in expression and finally pseudogenization of the ubiquitously expressed *GLDPB* copy during C_4 evolution eventually restricted glycine decarboxylase activity to bundle sheath-specific expression.

The genus *Moricandia* is closely related to *Arabidopsis*, which possesses two copies of the *GLDP* gene. The promoter region of the *AtGLDP1* gene contains *cis*-regulatory elements that govern expression in the mesophyll (M-box) and in the vasculature (V-box), respectively (1). Loss of the mesophyll element leads to a vein and bundle sheath-specific expression pattern of the *AtGLDP1*. The promoter of the second *AtGLDP2* gene contains an M-box but no V-box. Loss of the M-box in *AtGLDP1* would still be compensated by the function of *AtGLDP2* in *Arabidopsis* (1). However, in the subgroup of the Brassicaceae containing multiple C_3-C_4 evolutionary lineages in the genera *Moricandia*, *Diplotaxis*, and *Brassica*, the *GLDP2* gene copy was apparently lost (160). The promoter of the C_3 species in this Brassicaceae branch, e.g., *Moricandia moricandioides*, still contains both

regulatory elements (i.e., the V- and M-box), but the M-box element was lost from the *GLDP1* promoter of the C_3-C_4 intermediate species *M. nitens* and *M. arvensis*, resulting in bundle sheath-specific localization of the corresponding protein (1, 2).

These two examples show that in two phylogenetically distant plant families, C_3 relatives already contained a bundle sheath-specific *cis*-regulatory element in the promoter of the *GLDP* gene, thus facilitating the establishment of a glycine pump between mesophyll and bundle sheath cells in these lineages.

In the basic C_3-C_4 intermediate *M. arvensis*, strong bundle sheath specificity is apparently limited to the glycine decarboxylase P-protein (145). Other enzymes, such as the other subunits of the glycine decarboxylase system and serine hydroxymethyl transferase, are still present in the mesophyll. Serine, as the end product of the glycine decarboxylase reaction, could therefore be transported back to the mesophyll for further metabolization. In fully optimized C_4 species, all of the Rubisco resides in the bundle sheath, and the glycine shuttle is completely replaced by the more efficient C_4 pump.

Photorespiratory 2PG generation in C_4 plants is relatively low and also limited to the bundle sheath. In fully developed C_4 species, transcripts and proteins of the photorespiratory pathway are predominantly or exclusively found in the bundle sheath fraction. The only exception to this pattern is the last enzyme of the pathway, glycerate kinase, which is confined to the mesophyll cells in C_4 species of all decarboxylation types (**Figure 2**) (47, 182). Glycerate kinase catalyzes the conversion of glycerate to 3PGA and interconnects the photorespiratory pathway with the mesophyll part of the Calvin-Benson cycle. Due to the higher reductive power in the mesophyll cells, the reduction steps of the Calvin-Benson cycle are localized to the mesophyll cells connected to the bundle sheath part of the cycle by a 3PGA/trioseP shuttle (94, 129).

In contrast to C_3 and most other C_4 species, the glycerate kinase protein of maize carries a small C-terminal extension that is only present in Andropogonae C_4 species. It includes two cysteine residues that must be reduced for the activation of the enzyme in a light-dependent manner (15). Besides maize, thiol-mediated regulation of glycerate kinase was also found in the NADP-ME species sorghum but not in the NADP-ME dicot *Flaveria bidentis* (15). In the mesophyll cells of Andropogonae NADP-ME monocots, glycerate might therefore also serve as a carbon pool in the darkened leaf. At dawn, the activation of glycerate kinase would lead to the conversion of glycerate to 3PGA and thereby contribute to the buildup of the concentration gradients that drive the Calvin-Benson cycle intercellular shuttle (15).

Although the photorespiratory pathway runs at much lower rates in C_4 compared to C_3 species, the enzymes of the photorespiratory pathway are still essential (108, 205), and they need to be controlled in coordination with other pathways such as the Calvin-Benson cycle and nitrogen metabolism and need to adjust to the division of labor between the two cell types.

3.2. C_4 Fixation in Mesophyll Cells

Phospho*enol*pyruvate carboxylase (PEPC) catalyzes the irreversible reaction between bicarbonate and PEP, forming OAA and inorganic Pi. Once a photorespiratory glycine pump has evolved, any increases in the activity of PEPC in the mesophyll cells would enforce the production of the typical C_4 metabolites and intensify the exchange of metabolites between the cells (77, 115). This was convincingly demonstrated by increases in PEPC transcripts in leaves from different *Flaveria* species ranging from C_3 over different intermediate stages to the full C_4 pathway (56). C_4 leaves are generally characterized by very high activities of PEPC, and this activity is localized to the mesophyll cell cytosol. The abundance and cell specificity of the PEPC are particularly well-studied and have been found to happen on the epigenetic, transcriptional, and enzyme kinetic levels. Furthermore,

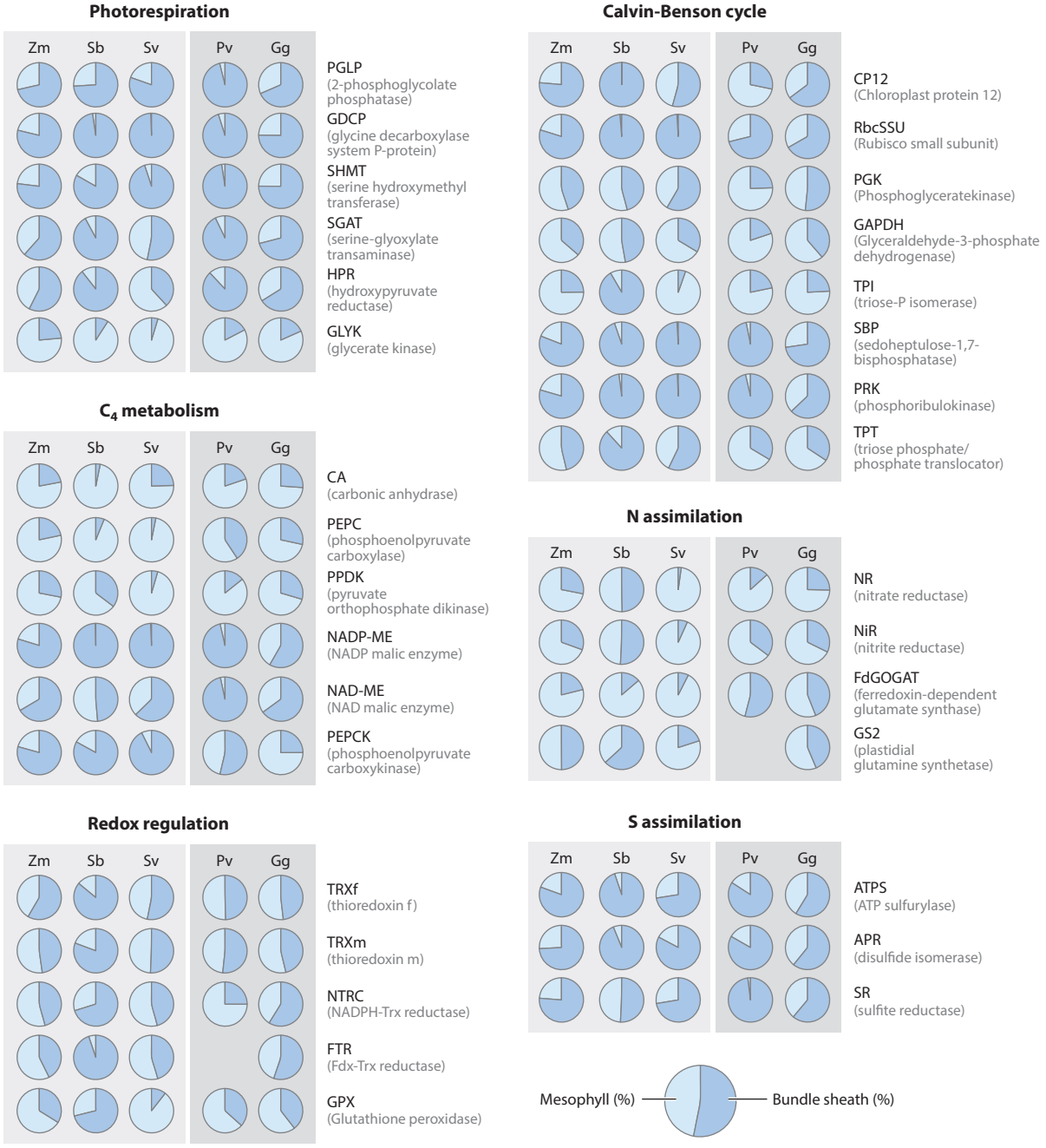

Figure 2

Distribution of transcript abundance between the mesophyll and bundle sheath in C_4 mature leaves. The pie charts show the percent of transcript isolated from mesophyll tissue (*light blue*) and bundle sheath (*dark blue*). The data are taken from studies in the NADP-ME grasses *Zea mays* (Zm; slice 1 = leaf tip from Reference 44), *Sorghum bicolor* (Sb; from Reference 47), and *Setaria viridis* (Sv; from Reference 86); the NAD-ME grass *Panicum virgatum* (Pv; from Reference 144) and the NAD-ME eudicot *Gynandropsis gynandra* (Gg; from Reference 12). Charts from species using the NADP-ME decarboxylation pathway are provided with light grey background, and charts for species using the NAD-ME decarboxylation pathway are provided with a darker grey background. Abbreviations: NAD-ME, NAD malic enzyme; NADP-ME, NADP malic enzyme.

PEPC and many other C_4 enzymes have co-opted regulatory mechanisms for the integration of their transcription into existing light- and plastid-regulated networks (28). Plant PEPCs are encoded by a small gene family, and certain gene copies have been preferred for integration into the C_4 pathway in the C_4 monocots (36). In the eudicots, two paralogous PEPC clades exist, and genes from both clades have been recruited to C_4 photosynthesis (151). Detailed sequence analyses showed that common sites of positive selection could be found in many of the C_4 PEPC genes, but that not all observed amino acid substitutions are essential for the C_4 pathway (151).

On the epigenetic level, PEPC expression is regulated by histone modifications and DNA methylation. High trimethylation of histone H3K4 confers increased transcription activity and has been associated specifically with regions in the *C4-Pepc* promoter in the mesophyll cells of the C_4 species *Z. mays*, *S. bicolor*, and *S. italica* (78). Similar cell-specific histone codes could also be found in other C_4 cycle genes, a mesophyll-specific modification of CA (*C4-Ca*) and PPDK (*C4-Ppdk*), and a bundle sheath-specific modification of NADP-ME (*C4-Me*) and PEPCK (*C4-Pepck*) (78). Additionally, mesophyll-specific accumulation of PEPC-encoding transcripts could be correlated to methylation sites in the promoter in maize (105). Gene transcription is further regulated by *cis* elements in the promoter that can be controlled by specific transcription factors. In the promoter region of the PEPC-encoding gene from *Flaveria trinervia*, two regions mediating mesophyll-specific expression could be identified, and one of these regions could be narrowed to a mesophyll-enhancing module (*MEM1*), with the tetranucleotide CACT as the key element (72). In *Flaveria bidentis*, interacting zinc finger-homeodomain (ZF-HD) homeobox proteins binding to the PEPC promoter region were identified (200). In maize, the transcription factor DOF1 seems to promote PEPC transcription throughout the leaf, while DOF2 specifically represses PEPC transcription in the bundle sheath (202). Also in maize, a 600-bp-long promoter region is sufficient to drive strong and light-activated expression in the mesophyll cells (117). Two transcription factors with antagonistic effects interact with this promoter region in maize. ZmbHLH90 activates while ZmbHLH80 represses expression of the PEPC-encoding gene, and the differential expression of these *trans*-factors contributes to the cell specificity of PEPC accumulation in maize (69).

On the metabolic level, PEPC activity is controlled by the availability of its substrates, bicarbonate and PEP. PEP availability is controlled by PPDK activity but also the interconversion between PEP and 3PGA (10, 45). Compared with C_3 PEPCs, enzymes from C_4 species require higher concentrations of the PEP substrate, and they are much less sensitive to inhibition by malate and aspartate (85), thus being adapted to the conditions in the C_4 mesophyll that contains high concentrations of PEP and malate or aspartate (56). The relaxation of the inhibitory effect of malate could be narrowed down to the exchange of a single amino acid. Close to the inhibitor binding site, C_3 species possess a bulky, positively charged arginine residue that is replaced by an uncharged and small glycine residue in C_4 species from very different plant groups, such as the dicot *Flaveria* and the grasses maize, sugarcane, and sorghum (139). In *Flaveria* the C_4-specific changes in PEP saturation kinetics also could be associated with a specific, single amino acid exchange in the carboxyl terminal part of the enzyme (18). In C_4 *Flaveria* species, PEPC shows a clear diurnal activity pattern in close coordination with the pattern for the PEPC kinase (4). The PEPC kinase itself is regulated on the transcriptional level and by protein synthesis/turnover (4).

CAs catalyze the conversion of CO_2 to bicarbonate and thus provide the substrate for the PEPC reaction. Members of the β-CA family therefore also show high activity in the cytosol of mesophyll cells of C_4 species. In C_3 plants, β-CAs are usually active in the plastids. Integration into the C_4 pathways is therefore dependent on increases in the activity as well as changes in localization toward the cytosol. In *Flaveria*, this is realized by the loss of the plastid targeting signal so that the C_4-specific CA becomes expressed in the cytoplasm (111). In *Gynandropsis gynandra*, C_4-related CA activity was realized by a membrane-bound CA, indicating that a different ancestral CA isoform

was recruited to C_4 in *Flaveria* (24, 111). In C_4 monocot species such as maize, C_4-related cytosolic CA activity was suggested to have evolved from ancestral plastidial forms by gene duplication, gene fusion, and changes in the chloroplast targeting signal (111). In addition, recruitment of CA into the C_4 pump was also accompanied by changes in the histone codes and integration into the light- and plastid-controlled signaling network. In *Flaveria*, mesophyll cell-specific expression was apparently realized by a structurally similar motif (*MEM1*) upstream of the transcription start site for CA and PEPC, indicating that high coordination for the presence of both initial C_4 enzymes is achieved in *Flaveria* (73). While a reduction of CA activity strongly reduced photosystem activity in C_4 *Flaveria* (185), even a 97% reduction of CA activity in maize resulted in a rather mild phenotype under ambient CO_2 conditions (172). Only under low CO_2 conditions that probably existed during C_4 evolution did the CA antisense maize display an appreciable growth phenotype (172).

PPDK provides the PEP for the PEPC reaction in the mesophyll cells of C_4 plants. The reaction is dependent on the provision of ATP and represents a rate-limiting step in the C_4 pathway (51). The ATP supply for the PPDK reaction is provided by enhanced cyclic electron flow in C_4 leaves (24, 71). During the PPDK reaction, ATP is cleaved into AMP and PPi. The regeneration into ADP and Pi is realized by AMP kinase and pyrophosphorylase, respectively. In C_3 as well as C_4 species the PPDK gene produces a cytosolic and plastidial form by using two different promoters; the promoter for the shorter cytosolic is situated in the first intron of the longer plastidial transcript (166). In C_4 plants, the plastidial PPDK is upregulated in the mesophyll cells. In maize and *Flaveria*, *cis*-acting promoter elements promote mesophyll-specific expression of the PPDK (118, 150). The sensitivity of PPDK to low temperatures was suggested as one explanation for the restriction of the majority of C_4 species to warmer climates. The chilling-tolerant C_4 species *Miscanthus* × *giganteus* displays significantly increased PPDK content and activity under low temperatures, thus stabilizing the C_4 pathway under these conditions (189). PPDK activity is controlled in a light-dependent manner by the PPDK regulatory protein (31). In maize, two copies of the PPDK regulatory protein with distinct function and cellular distribution exist. The bundle sheath-specific copy lacks PPDK-activating phosphotransferase activity, thus contributing to cell-specific PPDK activity (30).

For the transport of pyruvate into the mesophyll plastid, different mechanisms have been recruited into the C_4 cycle in different C_4 lineages. The majority of C_4 species use a BASS2/NHD/PPT transport system, which combines the exchange of pyruvate with sodium, sodium against protons, and phosphate against PEP (67). The Andropogonae, such as maize and sorghum, have been reported to exchange pyruvate for protons directly, without the involvement of a sodium gradient (8).

3.3. C_4 Shuttle Between Mesophyll and Bundle Sheath Cells

All C_4 lineages use CA, PEPC, and PPDK for the prefixation of atmospheric CO_2. The following reactions in the C_4 cycle, however, can vary and are mainly connected to the preferential decarboxylation type in the bundle sheath. In NADP-ME species, the OAA produced in the PEPC reaction is converted to malate by the plastidial NADP-MDH; malate diffuses to the bundle sheath chloroplast where it is decarboxylated by the NADP-ME-producing pyruvate, which needs to diffuse back to the mesophyll cell for regeneration of PEP. In NAD-ME species, OAA is transaminated into aspartate by the aspartate aminotransferase (AspAT). The reaction usually takes place in the cytosol of the mesophyll cell, but transcript data from *G. gynandra* indicate a mitochondrial localization of the enzyme (**Figure 1*b***) (159, 169). Aspartate diffuses to the bundle sheath where it enters the mitochondria and is transaminated back to OAA by the mitochondrial AspAT, followed by conversion into malate by the mitochondrial NAD-MDH. Malate is decarboxylated

in the mitochondria by NAD-ME; the pyruvate generated in the reaction is transaminated to pyruvate by the alanine aminotransferase (AlaAT) into alanine. The transport of alanine back to the mesophyll cell rebalances the nitrogen metabolism between the cells and can be reconverted back by the AlaAT to pyruvate for the regeneration of PEP. In the PEPCK subtype, the transport metabolites malate and aspartate are generated in the mesophyll cell as described above. After diffusion into the bundle sheath, the aspartate is transaminated by the cytosolic AspAT into OAA, followed by decarboxylation by the cytosolic PEPCK into PEP. The reaction is accompanied by the conversion of ATP to ADP and Pi. PEP can be transported back directly to the mesophyll cell where it can be used directly by PEPC. In order to balance the nitrogen metabolism between the mesophyll and bundle sheath cells, a second cycle is usually active in PEPCK species. Parallel to the aspartate, malate diffuses from the mesophyll to the bundle sheath cell where it is transported into the mitochondria for decarboxylation by NAD-ME. The produced pyruvate is transaminated by the AlaAT into alanine, which diffuses back into the mesophyll cell. Besides this combined PEPCK/NAD-ME system, considerable PEPCK activity has also been found in species with dominating NAD-ME or NADP-ME activity (141, 169). In the NADP-ME species maize, the PEPCK-related shuttle caries 10–14% of the carbon into the bundle sheath (10), and for the dicot NADP-ME *Flaveria* species, aspartate labeling of 30–40% has been estimated (122).

The transport of the shuttle metabolites between the mesophyll and bundle sheath cell depends on high metabolite concentrations to drive the diffusion. Estimations of the cell-specific metabolite pools in maize leaves yielded gradients in the expected directions with higher concentrations for malate, aspartate, and trioseP in the mesophyll cells and higher pools for alanine and 3PGA in the bundle sheath cells. Only for pyruvate did the estimated gradient not show the expected pattern. It is, however, possible that the buildup of the pyruvate gradient relies on subcellular compartmentation that was not accounted for in the analysis (10). The presence of multiple shuttles, such as the parallel malate and aspartate shuttles in maize, possibly increases the robustness of the C_4 shuttle because it permits the maintenance of photosynthesis at lower concentrations of each individual metabolite, especially under fluctuating environmental conditions (10, 141).

3.4. C_4 Decarboxylation in Bundle Sheath

The C_4 bundle sheath metabolism is largely influenced by the type and localization of the decarboxylating enzyme. The reasons for the recruitment of a particular decarboxylating enzyme into the C_4 metabolism of different lineages are not yet clear. It is possible that transcript abundance or enzyme kinetics played a role in the recruitment into C_4 (23). Comparisons of the physiology in grasses of the three different carboxylation types showed that NAD-ME species are more sensitive to low light conditions than NADP-ME and PEPCK species (170). NADP-ME species also seem to have higher nitrogen-use efficiencies than the other two subtypes (142). Modeling approaches indicated that light availability and distribution within the leaf could play important roles in the evolutionary choice of the decarboxylation type (19).

Individual C_4 lineages have acquired diverse control mechanisms for their decarboxylating enzymes. Sequence analysis of the NADP-ME encoding genes in two C_4 *Flaveria* species (*F. bidentis*, *F. trinervia*) revealed different regulatory mechanisms for the closely related but independently evolved C_4 lineages (102). In maize and sorghum, the C_4 NADP-ME encoding genes seem to have acquired increased binding capacity for a specific bHLH transcription factor by *cis* element duplication (21). In maize, duplication of these C_4-related bHLH transcription factors possibly contributed to the refined regulation of the enzyme (21). Additionally, NADP-ME was optimized for the C_4 environment by amino acid sequence modifications conferring changes in the catalytic activity, tetrameric structure, and pH-dependent inhibition by its substrate malate (7).

In the NAD-ME and PEPCK subtypes, aspartate and alanine are shuttled between the mesophyll and bundle sheath cells, and depending on the contribution of PEPCK, this type of shuttle is also active in the NADP-ME species. Recruitment of the AspAT to C_4 metabolism was thereby connected to the biochemical subtype. A plastidial AspAT was enhanced in the NADP-ME species, while mitochondrial and cytosolic isoforms were increased in NAD-ME lines. Predominant PEPCK decarboxylation was accompanied only by high cytosolic AspAT abundance (159). For the AlaAT, a cytosolic copy was upregulated in the monocot species. Since the branch encoding cytosolic AlaAT in monocots is missing in eudicots, C_4 photosynthesis recruited a gene copy from a mitochondrial branch (159).

The organellar localization of many C_4 enzymes requires cell- and metabolite-specific transport activities for completion of the C_4 cycle, but not all of the transport steps of the responsible proteins have been identified (161). In maize, the DiT1 chloroplast transporter facilitating malate export showed higher abundance in the mesophyll cells, while the malate-importing DiT2 transporter was enhanced in the bundle sheath fraction (114).

3.5. Calvin-Benson Cycle in C_4 Species

CO_2 enrichment in the bundle sheath of C_4 species allows a high carboxylation efficiency of Rubisco, and C_4 leaves contain significantly lower amounts of Rubisco, as compared to C_3 species. C_4 Rubisco has a higher catalytic turnover, and due to the high CO_2 environment it can work with lower CO_2 binding affinity (165). The changes in the expression pattern of Rubisco in C_4 species require coordination of the transcription of the nucleus-encoded genes for small subunits and the chloroplast-encoded large subunit genes. In C_3 plants Rubisco expression is already strongly influenced by developmental and environmental factors, especially light (17, 80). During very early stages of leaf development, genes for the Rubisco subunits are usually still expressed in both cell types. The subsequent restriction of Rubisco activity to the bundle sheath in C_4 species is then controlled on multiple, mainly posttranscriptional levels (17). In maize, cell-type-specific expression of the *rbcS-m3* gene seems to be dependent on light signaling (143). A zinc finger protein (TRM1) is then involved in the mesophyll-specific repression of the ZmRbcSm3 protein (201). In C_4 dicots, such as *Amaranthus hypochondriacus* and *F. bidentis*, sequences in the untranslated regions of the genes (*AhRbcS1* and *FbRbcS1*) seem to be important for the stability of the corresponding mRNA in the mesophyll cells (137, 138). The half-life of the plastid-encoded *rbcL* mRNA is generally connected to the presence of nucleus-encoded S1 domain RNA binding protein (RLSB), and during transition from C_3 to C_4 in *Flaveria* species, they were strongly coregulated (203).

The enzymatic complement of the Calvin-Benson cycle is the same in C_3 and C_4 species, but in C_4 species the Calvin-Benson cycle is split between the mesophyll and bundle sheath cells. Enzymes of the fixation and ribulose 1,5-bisphosphate regeneration phase are preferentially found in the bundle sheath. Only the reduction of 3PGA to trioseP that is catalyzed by the glyceraldehyde 3-phosphate dehydrogenase (GAPDH) and the triose phosphate isomerase is preferentially localized to the mesophyll in all C_4 subtypes (114) (**Figure 2**). C_4-specific modifications have also been detected in the Calvin-Benson cycle enzymes fructose 1,6-bisphosphate aldolase (FBA) and fructose 1,6-bisphosphate phosphatase (FBP) (82). In the maize leaf, two copies of *GAPDH* exist, and while *GAPDH-A* was equally distributed between both cell types, *GAPDH-B* preferentially accumulated in the mesophyll cells (114). The differential accumulation of Calvin-Benson cycle enzymes has been shown at the protein levels by separation of mesophyll and bundle sheath chloroplasts (65) as well as on the transcript level by differential analysis of mesophyll and bundle sheath transcriptomes in leaves of the NADP-ME species maize (29, 44, 109, 176), *S. bicolor* (47),

and *S. italica* (86), and in the NAD-ME species *Panicum virgatum* (144) and *G. gynandra* (12). Division of the Calvin-Benson cycle between the two cell types also requires the enhanced operation of the trioseP transporter (TPT) across the chloroplast membrane. Its transcripts are upregulated in both cell types, and compared to C_3 species, the transporters show modifications in their kinetics (114, 136).

Recently, an unbiased comparison of the Calvin-Benson cycle metabolite abundances in different C_3 and C_4 species clearly distinguished specific Calvin-Benson cycle metabolite patterns in the different photosynthesis types (9). The C_4 species had lower amounts of most Calvin-Benson cycle intermediates, especially ribulose 1,5-bisphosphate. However, 3PGA and trioseP were enhanced in the C_4 leaves, especially in the monocot species, and this could be connected to the high demand of these metabolites for the buildup of the metabolite gradient between the mesophyll and bundle sheath cells that are driving the metabolite exchange by diffusion (9).

3.6. Division of Photosystems in C_4

The flux trough the trioseP/3PGA shuttle is connected to the specific ATP/NADPH demand in the mesophyll and bundle sheath cells and could be subtype and lineage specific (129). In the NADP-ME species maize, NADPH in the mesophyll chloroplasts is needed for the reduction of OAA to malate. In the bundle sheath chloroplast, NADPH is released during oxidative decarboxylation of malate by NADP-ME. Demand for NADPH production is therefore low in bundle sheath cells of pure NADP-ME species (88). In the NADP-ME species *Flaveria*, the larger contribution of aspartate to the C_4 shuttle likely also requires some NADPH production by linear electron flow in the bundle sheath cells. In NAD-ME species, the C_4 shuttle is realized completely by aspartate, and the C_4 shuttle therefore does not contribute to the exchange of reducing power between the two cell types (122, 129). In PEPCK-type C_4 metabolism, the ATP/NADPH demand does not increase considerably (129).

Energy and reducing equivalents are provided in the leaf by light-driven electron transport through the photosystems. The linear electron flow through photosystem I and photosystem II provides ATP and NADPH, and the cyclic electron flow around photosystem I and the NADH dehydrogenase-like complex (NDH) or the proton regulation pathway (PRG5-PRGL1) contributes to ATP production without accumulation of NADPH. The demand for different ratios of ATP/NADPH can be adjusted by control of electron transport through the two photosystems.

In NADP-ME species, high abundance of photosystem I and photosystem II in the mesophyll cells provides ATP and NADPH by linear electron transport. The bundle sheath chloroplasts, however, are specialized for cyclic electron transport around photosystem I, producing only ATP. Maize bundle sheath chloroplasts show high accumulation of photosystem I and the NDH complex, but low accumulation of photosystem II and a very low degree of thylakoid membrane appression (granal stacking) (65, 98, 173). The distribution of photosystem-related transcripts shows clear preference for photosystem II in the mesophyll cells. The electron flow from photosystem I to either the ferredoxin:NADP(H) oxidoreductase (FNR) in the linear electron transport chain or the flow back to the membrane complexes in the cyclic electron flow is mediated by ferredoxins (Fds) (70). In maize leaves, different forms of Fds are present in the different cell types, and FdI could be associated with linear electron flow in the mesophyll cells, while FdII seems to almost exclusively transfer electrons in cyclic flow (70).

In NAD-ME species, NADH produced by the decarboxylation of malate in the bundle sheath mitochondria is regenerated to NAD^+ by the reduction of OAA to malate in the same compartment. That is, no net transfer of redox power from mesophyll to bundle sheath cell occurs in this C_4 type. The chloroplasts in the mesophyll and bundle sheath cells contain both photosystems,

indicating that both linear and cyclic electron transport are active. Thylakoid membrane appression is equally distributed between both cell types or even lower in the mesophyll cells (52). The photosystem-related transcripts are much more evenly distributed between mesophyll and bundle sheath cells in the examined NAD-ME species (**Figure 1*b***).

3.7. Redox Regulation in C_4 Carbon Metabolism

Coordination of leaf development and metabolism, especially under fluctuating environmental conditions, is mediated via signaling networks depending on reactive oxygen species (ROS) production and protein redox status. In C_4 leaves, the ROS and redox status can differ considerably in the mesophyll and bundle sheath cells, and cell-specific adjustments of these regulatory systems are needed (178). In the NADP-ME species maize, the mesophyll-specific localization of photosystem II complexes and the linear electron transport chain correlated with the accumulation of ROS detoxification systems in the mesophyll cells, including tocopherol biosynthesis, glutathione reductase, ascorbate peroxidase, dehydroascorbate reductase, and thiol peroxidases (65). Lower ROS production could also be responsible for the comparatively reduced DNA damage found in the DNA of bundle sheath cell organelles (100).

The ROS status is related to the redox status of thioredoxins (TRXs), a group of proteins that can transfer redox signals to target proteins by modification of cysteine residues. In the plastids, the reduction of TRX is mediated either by NADPH-Trx reductases (NTRCs) receiving reducing power from NADPH or via electron transport from reduced Fds through the Fdx-Trx reductases (FTRs), thereby receiving reducing power directly from photosynthesis. Both systems apparently interact in the regulation of enzymes of the central cellular metabolism. In maize leaves, most members of the TRX signaling system show preferential accumulation in the mesophyll cells (178). The bundle sheath cells, however, seem to be depleted of components from both TRX systems and other TRX-like proteins and glutathiones, including NTRCs, FTRs, and many TRXs (178).

The lack of many redox regulatory components in the bundle sheath cells is particularly puzzling because several redox-regulated Calvin-Benson cycle proteins are localized in the bundle sheath cells (131). GAPDH, phosphoribulokinase (PRK), FBPase, and SBPase are directly redox-activated by TRX, and further control of the Calvin-Benson cycle is mediated by the redox modulation of CP12 and Rubisco activase. More recently, all other enzymes of the Calvin-Benson cycle were identified as possible targets of TRX signaling, indicating that the fine-tuning of Calvin-Benson cycle control is much more complicated than described so far (123). Beside the Calvin-Benson cycle proteins, other bundle sheath-localized enzymes, such as ADP-glucose pyrophosphorylase (AGPase), a key enzyme for starch synthesis, are also regulated by the redox signaling system. In the bundle sheath cells of the NADP-ME species, the C_4 cycle would also require activity of the redox-regulated NADP-MDH in the bundle sheath chloroplast. It is so far unknown whether the regulatory mechanisms for these proteins are the same in C_3 and in the bundle sheath cells of NADP-ME C_4 species. Bundle sheath cells contain an m-type TRX that could be sufficient for enzyme activation in light; additionally, the TRX-like CDSP32 and ascorbate peroxidase may contribute to redox signaling in the bundle sheath cells (131, 178).

The fine-tuning of the C_4 reactions in the CO_2 pump in the mesophyll cells and carbon reduction in the bundle sheath cells are particularly important under fluctuating environmental conditions (96). The rate of CO_2 fixation by PEPC must exceed the rate of the Rubisco reaction because a part of the CO_2 generated by decarboxylation in bundle sheath cells will leak out again and would need to be fixed in a second PEPC reaction, costing additional ATP for PEP regeneration. Environmental fluctuations, such as light and temperature changes, drought, or nitrogen availability, could also cause imbalances between the pathways (48). The integrations of the C_4

shuttle into the regulatory network of the underlying C_3 metabolism are achieved by recruitment of light-dependent and plastid-signal-mediated regulatory elements into the C_4 shuttle genes, including the transporters TPT, DCT, BASS2, NHD, and PPT as well as the enzymes CA, NAD-ME, AspAT, and pyrophosphorylase (28). More problematic could be short-term acclimation to rapid fluctuations of light intensity. Comparisons between C_3 and C_4 species under fluctuating light conditions showed that C_4 photosynthesis was more affected than C_3 under these conditions (97). Activation of the Calvin-Benson cycle enzymes upon transition from dark to light or from low to high light conditions is highly dependent on the redox signaling system (132), and it is currently unclear how rapid light activation of bundle sheath-localized enzymes works in C_4 species. Additionally, the pools of C_4 cycle intermediates must build up to allow the C_4 shuttle to work at sufficient turnover rates (181).

3.8. Consequences of C_4 Metabolism on Associated Pathways

Because the concentrations of ATP, reducing equivalents, and other metabolites considerably differ between mesophyll and bundle sheath cells, all cellular processes need to be adjusted. Cell-specific preferences have been found for the reaction of sucrose and starch synthesis, of tricarboxylic acid cycle (TCA), and of nitrogen and sulfur fixation.

The Calvin-Benson cycle provides the substrate for the synthesis of sucrose and starch. Proteins and transcripts of the starch metabolism have all shown higher abundances in the bundle sheath, although under high CO_2 conditions starch accumulation was also observed in mesophyll cells of C_4 *Panicum*, indicating that mesophyll cells are in principle capable of accumulating transitory starch (177). Starch accumulation has also been observed in the bundle sheath of young leaves in many C_3 species, where it is thought to function as storage of energy and carbon for further growth (124). The ability to accumulate starch in the bundle sheath is supposed to be favorable for the evolution of C_4 photosynthesis. In the C_4 leaf, the Calvin-Benson cycle reactions producing the substrate for starch synthesis are localized in the bundle sheath. High concentrations of 3PGA in the bundle sheath would also allosterically activate the AGPase, one of the key enzymes for starch synthesis (68). Transcripts for sucrose metabolism are preferentially found in the mesophyll cells. TrioseP, the substrate for sucrose synthesis, is produced by the mesophyll-localized Calvin-Benson cycle reactions, but considerable parts of the trioseP must be returned to the bundle sheath for ribulose 1,5-biphosphate regeneration (106). Sucrose synthesis in the C_4 mesophyll cells should therefore be under tight control. Indeed, it was found that the affinity of maize FBPase for trioseP is one order of magnitude lower than in C_3 species, which contributes to allowing the buildup of the TrioseP concentration gradient (171). Differences between C_3 and C_4 grasses were recently also detected for sucrose transport from the bundle sheath into the veins. In contrast to the connection between mesophyll and bundle sheath cells, the plasmodesmata density is low between bundle sheath and phloem cells, and it was suggested that the SWEET13 transporter contributes to the apoplastic transport of sucrose between these cell types (55).

In the NAD-ME and also PEPCK species, the C_4 cycle continually generates pyruvate that needs to be prevented from entering the TCA cycle (25). The mitochondrial pyruvate dehydrogenase complex can be inhibited by reversible phosphorylation via the pyruvate dehydrogenase (PDH) kinase. In NAD-ME species, expression of the PDH kinase is enhanced (25) and shows bundle sheath specificity in *Panicum virgatum* and *G. gynandra*, but this does not seem to be the case in the NADP-ME species. Labeling experiments showed very low leakage of C_4 metabolites into the respiratory metabolism in illuminated maize leaves (10).

Nitrogen metabolism of the leaf is closely connected to photorespiration in C_3 species. An increase in environmental CO_2 resulted in the expected reduction of photorespiration but also a reduction in nitrogen assimilation in C_3 (20). It is thus expected that in the C_4 leaf, nitrogen

metabolism needs to be adjusted to the low photorespiratory rates. Assimilation of nitrate requires reducing power and enzymatic activities. Transcripts for nitrate reductase, nitrite reductase, and the Fd-GOGAT, as well as one copy of the GS1, are preferentially found in the mesophyll cells (65, 126) (**Figure 2**), where photosynthetic linear electron transport provides the reducing power. A second copy of GS1 with similarly high expression levels but bundle sheath-specific accumulation was found in the tested C_4 species. Because photorespiration, albeit at a low rate, is present in the C_4 bundle sheath and the expression of the glycine decarboxylase system is restricted to this cell type, ammonium assimilation would be required in the bundle sheath to cope with ammonia release from photorespiration.

In contrast to nitrogen metabolism, the first steps of sulphate assimilation, including ATP sulphurylase, APS reductase, and sulphite reductase, take place in the bundle sheath cells of C_4 species (29, 65, 95). The sulphide is incorporated into cysteine and transported into the mesophyll cell for the synthesis of glutathione (65, 195). The preference for sulphate reduction in the bundle sheath is not simple to explain since reducing power, especially in the NADP-ME species, is mainly supplied by the C_4 shuttle (195). The bundle sheath-specific localization of sulphur assimilation, however, might predate the evolution of C_4, and bundle sheath specificity in the pathways has also been found in C_3 species such as *Arabidopsis* (13). Bundle sheath-specific elements have recently been identified in the promoter of a low-affinity sulphur transporter (SULTR2;2) of *Arabidopsis*, and these elements were also active in the C_4 Asteraceae *F. bidentis*, showing that bundle sheath cells even in C_3 species are more specialized than previously assumed and that existing bundle sheath expression systems can be integrated into C_4 species during evolution (93).

4. IMPLEMENTATION OF C_4 LEAF ANATOMY

The evolution of the biochemical C_4 pathways is strongly connected to changes in the anatomy of the leaf (for a recent review, see 164). The anatomy of the C_4 leaf provides the structural basis for separation of the PEPC and Rubisco fixation reactions while allowing for high fluxes of metabolite exchange. Variation exists also among the Kranz anatomy of different C_4 species regarding the number of bundle sheath layers around a vein, presence or absence of a mestome sheath, formation of a suberin layer, chloroplast positioning, and chloroplast dimorphism (164). Besides Kranz anatomy, specific forms of C_4 anatomy have been found in succulent species of the Chenopodiaceae where bands of mesophyll and bundle sheath cells are arranged around a central water storage and vein tissue (52). The leaves of single-cell C_4 species are characterized by very large cells with dimorphic plastids. These plastids harbor either primary or secondary CO_2 fixation reactions and are arranged at opposite cell sides or at the outer border of the cell versus the central compartment of the cell (186).

In the large majority of C_4 species, leaf anatomy is characterized by two concentric layers of mesophyll and bundle sheath cells around the leaf vasculature. This leads to high vein density and a stereotypical leaf architecture consisting of vein-bundle sheath cell-mesophyll cell-mesophyll cell-bundle sheath cell-vein (V-BS-M-M-BS-V). Hence, every mesophyll cell is in physical contact with a bundle sheath cell, an absolute requirement for the function of efficient C_4 biochemistry. In comparison to C_3 leaves, bundle sheath cells in C_4 species occupy a larger share of the leaf cross-sectional area, they contain more chloroplasts and other organelles, and their cell walls are often thickened. It has long been suggested that certain architectural preconditions are necessary in C_3 leaves for the evolution of C_4 biochemistry (156). Among the grasses, two large clades can be distinguished: the BEP (Bambusoideae, Ehrhartoideae, and Pooideae) and the PACMAD (Panicoideae, Arundinoideae, Chloridoideae, Micrairoideae, Aristidoideae and

Danthonioideae) clade. While C_4 evolution had been frequent within the PACMAD clade, to our knowledge it is absent from the BEP clade. Large-scale analysis of leaf anatomy traits showed that high rates of C_4 evolution could be associated with a high proportion of bundle sheath tissue in the leaves resulting from short distances between the bundle sheath and a large cross-sectional area of bundle sheath cells (34). These results support the hypothesis that anatomic enablers can promote or prevent C_4 evolution in certain plant groups.

As shown above, C_4 biochemistry requires high fluxes of metabolites between the mesophyll and bundle sheath cells, including the C_4-related carbon shuttle, the 3PGA/trioseP shuttle of the Calvin-Benson cycle, and translocation of glycerate from the photorespiratory pathway. Recent advances in the development of new clearing techniques together with three-dimensional immunolabeling confocal microscopy allowed detailed comparisons of the symplastic connectivity between mesophyll and bundle sheath cells in C_3 and C_4 grasses. Plasmodesmata density at the mesophyll-bundle sheath interface was up to nine times higher in C_4 grasses compared to C_4 leaves (41). This was due to increases in the number of plasmodesmata per pitfield area, as well as increased pitfield density at the interfaces in NADP-ME and PEPCK species. In NAD-ME grasses, plasmodesmata density was increased by larger pitfield area only (42). Also noticeable was the increased bundle sheath surface area to leaf area ratio in all C_4 leaves (42). Recent work with a *Setaria viridis* line displaying reduced PEPC activity showed increased stomata density between mesophyll and bundle sheath cells, and it has been speculated that the plasmodesmata density is actually responsive to changes in the C_4 photosynthetic flux (6).

The key proteins involved in C_4 biochemistry could be identified due to their high activity and their high protein and transcript abundance in the leaf tissue. The identification of factors that control the C_4 specific architecture is much more difficult. Forward genetics screening resulted in only a handful of interesting mutants, indicating that the construction of C_4 anatomy is highly complex and possibly characterized by redundancy (103). In maize, two mutants with bundle sheath-specific defects could be identified. In the *bsd1* mutant, the G2 transcription factor is lost (76, 104), and the *bsd2* mutant was affected in the assembly and stabilization of bundle sheath Rubisco (27, 152). In the *high chlorophyll fluorescence mutant 136* (*hcf136*), disturbance in the stabilization of the photosystem II caused mesophyll-specific defects (39). In rice, mutants with increased vein density could be isolated. They displayed enhanced photosynthetic rates, but the molecular mechanisms behind the architectural changes were not identified (59).

Early anatomical studies had already recognized some similarities between the endodermis of the root and the bundle sheath of the leaf. C_4-related features, such as high activities of decarboxylating enzymes, were also detected in the cells surrounding the vein in C_3 tobacco (81). The GRAS transcription factors SCARECROW (SCR) and SHORT ROOT (SHR) regulating the organization of the root endodermis were therefore tested for their possible involvement in the control in C_4 bundle sheath structure (63, 103, 168). Genes encoding both transcription factors are upregulated during vascular development in maize leaves (192), and mutation in the *Scr* gene resulted in disturbed bundle sheath chloroplast development, vein disorientation, and reduced vein density in maize leaves (168). Recent work in maize, however, identified a second copy of the *ZmSCR1* gene (*ZmSCR1b*), and analysis of the single and double *Zmscr* mutants indicates a role of the transcription factor in mesophyll cell development (83).

Genome-wide transcriptome sequencing experiments were recently applied to the search for regulators of C_4-specific anatomical features. In contrast to the genes for C_4 biochemistry, developmental regulators are expressed in low abundance and often only at specific stages and in specific cells. Their identification is therefore much more difficult than that of abundant enzymes in C_4 biochemistry. The transcriptome pattern along a developmental gradient (**Supplemental Table 1**) had been investigated in the NADP-ME species *Z. mays* (44, 109, 141, 176, 192, 204)

Supplemental Material >

and *Flaveria* (101, 115), as well as the NAD-ME species *G. gynandra* (12, 99). Mesophyll- and bundle sheath-specific transcriptomes have been investigated in the NADP-ME grasses maize (29, 44, 109, 176), *S. bicolor* (47), and *S. italica* (86) and the NAD-ME species *P. virgatum* (144) and *G. gynandra* (12). The transcript comparisons identified candidate regulators with transcript patterns associated with certain developmental stages, cell-type specific expression, or other C_4-related processes.

In *G. gynandra*, the differentiation of enlarged bundle sheath cells in the mature leaf could be associated with changes in the transcript pattern of cell cycle genes. In comparison with the leaf development in the related C_3 species *Tarenaya hassleriana*, the differentiation of mesophyll and bundle sheath cells was generally retarded in the C_4 leaf. An inhibitor of endoreduplication (GTL1) was expressed more highly at the later stages of leaf development in C_4 but not in C_3 species, indicating that endoreduplication was less suppressed in the mature leaf of C_4 species. In the same developmental stages, a bundle sheath-specific increase in nucleus size and increases in cells with high ploidy level could be detected in the *G. gynandra* leaf (99).

The most detailed data sets of leaf developmental transcriptome patterns exist for maize. Besides the developmental stages along the mature leaf, transcriptome patterns have also been studied in leaf primordia of foliar and husk leaves (192). In contrast to foliar leaves, husk leaves surrounding the female inflorescences are characterized by increased mesophyll cell numbers between the veins. All of these studies resulted in lists of genes, mainly transcription factors, with predicted function in the setup of Kranz anatomy. The overlap between the candidate lists from different experiments had been limited, but transcription factors with potential mesophyll- or bundle sheath-specific activity could be identified in multiple studies (**Supplemental Table 2**). From the list of Wang and colleagues (192), 60 transcription factors with possible positive regulatory function toward Kranz anatomy have been tested by transformation into rice, but none of these genes were individually sufficient to induce C_4-like anatomy into rice (191). A large group of the candidate regulators had no phenotype; others affected the leaf hormone metabolism or perturbed the root/shoot development or cell formation (191). The most promising results have been obtained from overexpression of the maize G2-like (*GLK*) transcription factors in rice (193). GLK transcription factors also regulate chloroplast development in C_3 monocot and dicot species (12), but overexpression of the *OsGLK1* gene in rice influenced chloroplast development only at the young seedling stage (130). Constitutive expression of the *ZmGLK* genes in rice now induced chloroplast and mitochondria development in the cells surrounding the veins, but not in the mesophyll cells. The increased organelle volume was accompanied by an increased number of plasmodesmata between mesophyll and bundle sheath cells. The results show that *trans*-regulation of several C_4-like features is possible (193). Large-scale analysis of transcript patterns along early maize seedling development was recently used for the identification of *cis* elements in groups of coexpressed genes and the prediction of their interaction with coexpressed transcription factors (204). The engineering of C_4 pathways into C_3 species will largely depend on the ability to understand and implement the regulatory elements conferring C_4-like leaf anatomy.

SUMMARY POINTS

1. The large majority of changes to C_3 photosynthetic metabolism during the evolution of C_4 photosynthesis occurred gradually, by small successive changes driven by small fitness gains in the direction of C_4, e.g., by the improvement of nitrogen balancing between

cells, increases in bundle sheath decarboxylation activity, increases in C_4 production in the mesophyll, relocation of Rubisco activity to the bundle sheath, and adjustment of leaf architecture by increases in vein density, bundle sheath activity, and intercellular connectivity. Many of the regulatory changes occur by the capture of regulatory elements that are already present in C_3.

2. In addition to the changes in regulation manifested at the genomic level of C_4 species, efficient C_4 photosynthesis is probably also supported by regulatory systems that already confer flexibility in C_3 species. The activity of enzymes could thereby respond to changes in the redox balance and subsequent signaling pathways of a cell under C_4 conditions. The availability of high redox power in mesophyll cells, for instance, could activate specific processes and thereby drive their cell specificity.
3. With the exception of the reaction for CO_2 prefixation and PEP regeneration, various solutions have evolved in different C_4 lineages, most prominently in the evolution of different decarboxylation types.
4. The different decarboxylation schemes entail specific changes in the interconnecting steps for the CO_2 pump and the specific metabolic environment created in the mesophyll and bundle sheath cells.
5. Overlap in the recruitment of specific elements into the regulation of C_4 was found (e.g., light- and plastid-regulated elements). However, for many additional regulatory steps, individual solutions evolved in the different lineages. Hence, opportunities for the identification of regulatory elements through the comparison of multiple C_4 lineages might be limited.

FUTURE ISSUES

1. Regarding the thiol-based regulation of Calvin-Benson cycle enzymes in bundle sheath of nicotinamide adenine dinucleotide phosphate malic enzyme (NADP-ME) C_4 species, How does redox regulation work in the absence of linear photosynthetic electron transport in this cell type?
2. How is acclimation to rapidly fluctuating light conditions achieved and regulated in C_4 plants?
3. Do photorespiratory metabolites such as glycerate serve as reserve carbon pools for the replenishing of the Calvin-Benson cycle during dark-to-light transition and under fluctuating light conditions?
4. What is the contribution of parallel decarboxylation pathways in achieving robustness to environmental fluctuations in C_4?
5. How is Kranz anatomy regulated?

DISCLOSURE STATEMENT

The authors are not aware of any affiliations, memberships, funding, or financial holdings that might be perceived as affecting the objectivity of this review.

ACKNOWLEDGMENTS

This work was funded by the Deutsche Forschungsgemeinschaft (DFG, German Research Foundation) under Germany's Excellence Strategy EXC-2048/1, Project ID 390686111, and ERA-CAPS project C4BREED (WE 2231/20-1). We dedicate this review to the memory of Udo Gowik.

LITERATURE CITED

1. Adwy W, Laxa M, Peterhansel C. 2015. A simple mechanism for the establishment of C_2-specific gene expression in Brassicaceae. *Plant J.* 84(6):1231–38
2. Adwy W, Schlüter U, Papenbrock J, Peterhansel C, Offermann S. 2019. Loss of the M-box from the glycine decarboxylase P-subunit promoter in C2 *Moricandia* species. *Plant Gene* 18:100176
3. Agetsuma M, Furumoto T, Yanagisawa S, Izui K. 2005. The ubiquitin-proteasome pathway is involved in rapid degradation of phosphoenolpyruvate carboxylase kinase for C_4 photosynthesis. *Plant Cell Physiol.* 46(3):389–98
4. Aldous SH, Weise SE, Sharkey TD, Waldera-Lupa DM, Stuhler K, et al. 2014. Evolution of the phospho*enol*pyruvate carboxylase protein kinase family in C_3 and C_4 *Flaveria* spp. *Plant Physiol.* 165(3):1076–91
5. Ali S, Taylor WC. 2001. Quantitative regulation of the Flaveria Me1 gene is controlled by the 3′-untranslated region and sequences near the amino terminus. *Plant Mol. Biol.* 46(3):251–61
6. Alonso-Cantabrana H, Cousins AB, Danila F, Ryan T, Sharwood RE, et al. 2018. Diffusion of CO_2 across the mesophyll-bundle sheath cell interface in a C_4 plant with genetically reduced PEP carboxylase activity. *Plant Physiol.* 178(1):72–81
7. Alvarez CE, Bovdilova A, Höppner A, Wolff C-C, Saigo M, et al. 2019. Molecular adaptations of NADP-malic enzyme for its function in C_4 photosynthesis in grasses. *Nat. Plants* 5:755–65
8. Aoki N, Ohnishi J, Kanai R. 1992. Two different mechanisms for transport of pyruvate into mesophyll chloroplasts of C_4 plants—a comparative study. *Plant Cell Physiol.* 33:805–9
9. Arrivault S, Alexandre Moraes T, Obata T, Medeiros DB, Fernie AR, et al. 2019. Metabolite profiles reveal interspecific variation in operation of the Calvin-Benson cycle in both C_4 and C_3 plants. *J. Exp. Bot.* 70(6):1843–58
10. Arrivault S, Obata T, Szecówka M, Mengin V, Guenther M, et al. 2017. Metabolite pools and carbon flow during C_4 photosynthesis in maize: $^{13}CO_2$ labeling kinetics and cell type fractionation. *J. Exp. Bot.* 68(2):283–98
11. Aubry S, Brown NJ, Hibberd JM. 2011. The role of proteins in C_3 plants prior to their recruitment into the C_4 pathway. *J. Exp. Bot.* 62(9):3049–59
12. Aubry S, Kelly S, Kümpers BMC, Smith-Unna RD, Hibberd JM. 2014. Deep evolutionary comparison of gene expression identifies parallel recruitment of *trans*-factors in two independent origins of C_4 photosynthesis. *PLOS Genet.* 10(6):e1004365
13. Aubry S, Smith-Unna RD, Boursnell CM, Kopriva S, Hibberd JM. 2014. Transcript residency on ribosomes reveals a key role for the *Arabidopsis thaliana* bundle sheath in sulfur and glucosinolate metabolism. *Plant J.* 78(4):659–73
14. Bansal KC, Viret JF, Haley J, Khan BM, Schantz R, Bogorad L. 1992. Transient expression from cab-m1 and rbcS-m3 promoter sequences is different in mesophyll and bundle sheath cells in maize leaves. *PNAS* 89(8):3654–58
15. Bartsch O, Mikkat S, Hagemann M, Bauwe H. 2010. An autoinhibitory domain confers redox regulation to maize glycerate kinase. *Plant Physiol.* 153(2):832–40
16. Bellasio C, Farquhar GD. 2019. A leaf-level biochemical model simulating the introduction of C_2 and C_4 photosynthesis in C_3 rice: gains, losses and metabolite fluxes. *New Phytol.* 223(1):150–66
17. Berry JO, Mure CM, Yerramsetty P. 2016. Regulation of Rubisco gene expression in C_4 plants. *Curr. Opin. Plant Biol.* 31:23–28

18. Bläsing OE, Westhoff P, Svensson P. 2000. Evolution of C_4 phosphoenolpyruvate carboxylase in *Flaveria*, a conserved serine residue in the carboxyl-terminal part of the enzyme is a major determinant for C_4-specific characteristics. *J. Biol. Chem.* 275(36):27917–23
19. Blätke M-A, Bräutigam A. 2019. Evolution of C_4 photosynthesis predicted by constraint-based modelling. *eLife* 8:e49305
20. Bloom AJ. 2015. Photorespiration and nitrate assimilation: a major intersection between plant carbon and nitrogen. *Photosynth. Res.* 123(2):117–28
21. Borba AR, Serra TS, Górska A, Gouveia P, Cordeiro AM, et al. 2018. Synergistic binding of bHLH transcription factors to the promoter of the maize *NADP-ME* gene used in C_4 photosynthesis is based on an ancient code found in the ancestral C_3 state. *Mol. Biol. Evol.* 35(7):1690–705
22. Bowman SM, Patel M, Yerramsetty P, Mure CM, Zielinski AM, et al. 2013. A novel RNA binding protein affects *rbc*L gene expression and is specific to bundle sheath chloroplasts in C_4 plants. *BMC Plant Biol.* 13(1):138
23. Bräutigam A, Gowik U. 2016. Photorespiration connects C_3 and C_4 photosynthesis. *J. Exp. Bot.* 67(10):2953–62
24. Bräutigam A, Kajala K, Wullenweber J, Sommer M, Gagneul D, et al. 2011. An mRNA blueprint for C_4 photosynthesis derived from comparative transcriptomics of closely related C_3 and C_4 species. *Plant Physiol.* 155(1):142–56
25. Bräutigam A, Schliesky S, Külahoglu C, Osborne CP, Weber APM. 2014. Towards an integrative model of C_4 photosynthetic subtypes: insights from comparative transcriptome analysis of NAD-ME, NADP-ME, and PEP-CK C_4 species. *J. Exp. Bot.* 65(13):3579–93
26. Brown NJ, Newell CA, Stanley S, Chen JE, Perrin AJ, et al. 2011. Independent and parallel recruitment of preexisting mechanisms underlying C_4 photosynthesis *Science* (331):1436–39
27. Brutnell TP, Sawers RJ, Mant A, Langdale JA. 1999. BUNDLE SHEATH DEFECTIVE2, a novel protein required for post-translational regulation of the *rbc*L gene of maize. *Plant Cell* 11(5):849–64
28. Burgess SJ, Granero-Moya I, Grangé-Guermente MJ, Boursnell C, Terry MJ, Hibberd JM. 2016. Ancestral light and chloroplast regulation form the foundations for C_4 gene expression. *Nat. Plants* 2(11):16161
29. Chang Y-M, Liu W-Y, Shih AC-C, Shen M-N, Lu C-H, et al. 2012. Characterizing regulatory and functional differentiation between maize mesophyll and bundle sheath cells by transcriptomic analysis. *Plant Physiol.* 160(1):165–77
30. Chastain CJ, Baird LM, Walker MT, Bergman CC, Novbatova GT, et al. 2018. Maize leaf PPDK regulatory protein isoform-2 is specific to bundle sheath chloroplasts and paradoxically lacks a Pi-dependent PPDK activation activity. *J. Exp. Bot.* 69(5):1171–81
31. Chastain CJ, Failing CJ, Manandhar L, Zimmerman MA, Lakner MM, Nguyen THT. 2011. Functional evolution of C_4 pyruvate, orthophosphate dikinase. *J. Exp. Bot.* 62(9):3083–91
32. Chen T, Zhu XG, Lin Y. 2014. Major alterations in transcript profiles between C_3–C_4 and C_4 photosynthesis of an amphibious species *Eleocharis baldwinii*. *Plant Mol. Biol.* 86(1–2):93–110
33. Christin P-A, Boxall SF, Gregory R, Edwards EJ, Hartwell J, Osborne CP. 2013. Parallel recruitment of multiple genes into C_4 photosynthesis. *Genome Biol. Evol.* 5(11):2174–87
34. Christin P-A, Osborne CP, Chatelet DS, Columbus JT, Besnard G, et al. 2013. Anatomical enablers and the evolution of C_4 photosynthesis in grasses. *PNAS* 110(4):1381–86
35. Christin P-A, Sage TL, Edwards EJ, Ogburn RM, Khoshravesh R, Sage RF. 2011. Complex evolutionary transitions and the significance of C_3–C_4 intermediate forms of photosynthesis in Molluginaceae. *Evolution* 65(3):643–60
36. Christin P-A, Salamin N, Savolainen V, Duvall MR, Besnard G. 2007. C_4 photosynthesis evolved in grasses via parallel adaptive genetic changes. *Curr. Biol.* 17(14):1241–47
37. Christin P-A, Wallace MJ, Clayton H, Edwards EJ, Furbank RT, et al. 2012. Multiple photosynthetic transitions, polyploidy, and lateral gene transfer in the grass subtribe Neurachninae. *J. Exp. Bot.* 63(17):6297–308
38. Clayton H, Saladié M, Rolland V, Sharwood R, Macfarlane T, Ludwig M. 2017. Loss of the chloroplast transit peptide from an ancestral C_3 carbonic anhydrase is associated with C_4 evolution in the grass genus *Neurachne*. *Plant Physiol.* 173(3):1648–58

39. Covshoff S, Majeran W, Liu P, Kolkman JM, van Wijk KJ, Brutnell TP. 2008. Deregulation of maize C_4 photosynthetic development in a mesophyll cell-defective mutant. *Plant Physiol.* 146(4):1469–81
40. Covshoff S, Szecowka M, Hughes TE, Smith-Unna R, Kelly S, et al. 2016. C_4 photosynthesis in the rice paddy: insights from the noxious weed *Echinochloa glabrescens*. *Plant Physiol.* 170(1):57–73
41. Danila FR, Quick WP, White RG, Furbank RT, von Caemmerer S. 2016. The metabolite pathway between bundle sheath and mesophyll: quantification of plasmodesmata in leaves of C_3 and C_4 monocots. *Plant Cell* 28(6):1461–71
42. Danila FR, Quick WP, White RG, Kelly S, von Caemmerer S, Furbank RT. 2018. Multiple mechanisms for enhanced plasmodesmata density in disparate subtypes of C_4 grasses. *J. Exp. Bot.* 69(5):1135–45
43. Danker T, Dreesen B, Offermann S, Horst I, Peterhänsel C. 2008. Developmental information but not promoter activity controls the methylation state of histone H3 lysine 4 on two photosynthetic genes in maize. *Plant J.* 53(3):465–74
44. Denton AK, Maß J, Külahoglu C, Lercher MJ, Bräutigam A, Weber APM. 2017. Freeze-quenched maize mesophyll and bundle sheath separation uncovers bias in previous tissue-specific RNA-Seq data. *J. Exp. Bot.* 68(2):147–60
45. Doncaster HD, Leegood RC. 1987. Regulation of phosphoenolpyruvate carboxylase activity in maize leaves. *Plant Physiol.* 84(1):82–87
46. Dong X-m, Li Y, Chao Q, Shen J, Gong X-j, et al. 2016. Analysis of gene expression and histone modification between C_4 and non-C_4 homologous genes of *PPDK* and *PCK* in maize. *Photosynth. Res.* 129(1):71–83
47. Döring F, Streubel M, Bräutigam A, Gowik U. 2016. Most photorespiratory genes are preferentially expressed in the bundle sheath cells of the C_4 grass *Sorghum bicolor*. *J. Exp. Bot.* 67(10):3053–64
48. Driever SM, Kromdijk J. 2013. Will C_3 crops enhanced with the C_4 CO_2-concentrating mechanism live up to their full potential (yield)? *J. Exp. Bot.* 64(13):3925–35
49. Dunning LT, Olofsson JK, Parisod C, Choudhury RR, Moreno-Villena JJ, et al. 2019. Lateral transfers of large DNA fragments spread functional genes among grasses. *PNAS* 116(10):4416–25
50. Edwards EJ. 2014. The inevitability of C_4 photosynthesis. *eLife* 3:e03702
51. Edwards GE, Nakamoto H, Burnell JN, Hatch MD. 1985. Pyruvate,Pi dikinase and NADP-malate dehydrogenase in C_4 photosynthesis: properties and mechanism of light/dark regulation. *Ann. Rev. Plant Physiol.* 36:255–86
52. Edwards GE, Voznesenskaya EV. 2011. C_4 photosynthesis: Kranz forms and single cell in terrestrial plants. In *C_4 Photosynthesis and Related CO_2 Concentrating Mechanisms*, ed. AS Raghavendra, RF Sage, pp. 29–61. Dordrecht, Neth.: Springer
53. Ehleringer JR, Sage RF, Flanagan LB, Pearcy RW. 1991. Climate change and the evolution of C_4 photosynthesis. *Trends Ecol. Evol.* 6(3):95–99
54. Eisenhut M, Ruth W, Haimovich M, Bauwe H, Kaplan A, Hagemann M. 2008. The photorespiratory glycolate metabolism is essential for cyanobacteria and might have been conveyed endosymbiontically to plants. *PNAS* 105(44):17199–204
55. Emms DM, Covshoff S, Hibberd JM, Kelly S. 2016. Independent and parallel evolution of new genes by gene duplication in two origins of C_4 photosynthesis provides new insight into the mechanism of phloem loading in C_4 species. *Mol. Biol. Evol.* 33(7):1796–806
56. Engelmann S, Bläsing OE, Gowik U, Svensson P, Westhoff P. 2003. Molecular evolution of C_4 phospho*enol*pyruvate carboxylase in the genus *Flaveria*–a gradual increase from C_3 to C_4 characteristics. *Planta* 217(5):717–25
57. Esau K. 1943. Ontogeny of the vascular bundle in *Zea mays*. *Hilgardia* 15(3):327–68
58. Fankhauser N, Aubry S. 2017. Post-transcriptional regulation of photosynthetic genes is a key driver of C_4 leaf ontogeny. *J. Exp. Bot.* 68(2):137–46
59. Feldman AB, Murchie EH, Leung H, Baraoidan M, Coe R, et al. 2014. Increasing leaf vein density by mutagenesis: laying the foundations for C_4 rice. *PLOS ONE* 9(4):e94947
60. Fischer WW, Hemp J, Johnson JE. 2016. Evolution of oxygenic photosynthesis. *Annu. Rev. Earth Planet. Sci.* 44:647–83

61. Fisher AE, McDade LA, Kiel CA, Khoshravesh R, Johnson MA, et al. 2015. Evolutionary history of *Blepharis* (Acanthaceae) and the origin of C_4 photosynthesis in section *Acanthodium*. *Int. J. Plant Sci.* 176(8):770–90
62. Flügel F, Timm S, Arrivault S, Florian A, Stitt M, et al. 2017. The photorespiratory metabolite 2-phosphoglycolate regulates photosynthesis and starch accumulation in Arabidopsis. *Plant Cell* 29(10):2537–51
63. Fouracre JP, Ando S, Langdale JA. 2014. Cracking the Kranz enigma with systems biology. *J. Exp. Bot.* 65(13):3327–39
64. Freitag H, Kadereit G. 2014. C_3 and C_4 leaf anatomy types in Camphorosmeae (Camphorosmoideae, Chenopodiaceae). *Plant Syst. Evol.* 300(4):665–87
65. Friso G, Majeran W, Huang M, Sun Q, van Wijk KJ. 2010. Reconstruction of metabolic pathways, protein expression, and homeostasis machineries across maize bundle sheath and mesophyll chloroplasts: large-scale quantitative proteomics using the first maize genome assembly. *Plant Physiol.* 152(3):1219–50
66. Furbank RT. 2011. Evolution of the C_4 photosynthetic mechanism: Are there really three C_4 acid decarboxylation types? *J. Exp. Bot.* 62(9):3103–8
67. Furumoto T, Yamaguchi T, Ohshima-Ichie Y, Nakamura M, Tsuchida-Iwata Y, et al. 2011. A plastidial sodium-dependent pyruvate transporter. *Nature* 476(7361):472–76
68. Geigenberger P. 2011. Regulation of starch biosynthesis in response to a fluctuating environment. *Plant Physiol.* 155(4):1566–77
69. Górska AM, Gouveia P, Borba AR, Zimmermann A, Serra TS, et al. 2019. ZmbHLH80 and ZmbHLH90 transcription factors act antagonistically and contribute to regulate *PEPC1* cell-specific gene expression in maize. *Plant J.* 99(2):270–85
70. Goss T, Hanke G. 2014. The end of the line: Can ferredoxin and ferredoxin NADP(H) oxidoreductase determine the fate of photosynthetic electrons? *Curr. Protein Pept. Sci.* 15(4):385–93
71. Gowik U, Bräutigam A, Weber KL, Weber APM, Westhoff P. 2011. Evolution of C_4 photosynthesis in the genus *Flaveria*: How many and which genes does it take to make C_4? *Plant Cell* 23(6):2087–105
72. Gowik U, Burscheidt J, Akyildiz M, Schlue U, Koczor M, et al. 2004. *cis*-Regulatory elements for mesophyll-specific gene expression in the C_4 plant *Flaveria trinervia*, the promoter of the C_4 phosphoenolpyruvate carboxylase gene. *Plant Cell* 16(5):1077–90
73. Gowik U, Schulze S, Saladié M, Rolland V, Tanz SK, et al. 2017. A MEM1-like motif directs mesophyll cell-specific expression of the gene encoding the C_4 carbonic anhydrase in *Flaveria*. *J. Exp. Bot.* 68(2):311–20
74. Haberlandt G. 1896. *Physiologische Pflanzenanatomie*. Leipzig, Ger.: Wilhelm Engelmann
75. Hagemann M, Weber APM, Eisenhut M. 2016. Photorespiration: origins and metabolic integration in interacting compartments. *J. Exp. Bot.* 67(10):2915–18
76. Hall LN, Rossini L, Cribb L, Langdale JA. 1998. GOLDEN 2: a novel transcriptional regulator of cellular differentiation in the maize leaf. *Plant Cell* 10(6):925–36
77. Heckmann D, Schulze S, Denton A, Gowik U, Westhoff P, et al. 2013. Predicting C_4 photosynthesis evolution: modular, individually adaptive steps on a Mount Fuji fitness landscape. *Cell* 153(7):1579–88
78. Heimann L, Horst I, Perduns R, Dreesen B, Offermann S, Peterhansel C. 2013. A common histone modification code on C_4 genes in maize and its conservation in sorghum and *Setaria italica*. *Plant Physiol.* 162(1):456–69
79. Hennacy JH, Jonikas MC. 2020. Prospects for engineering biophysical CO_2 concentrating mechanisms into land plants to enhance yields. *Ann. Rev. Plant Biol.* 71:461–85
80. Hibberd JM, Covshoff S. 2010. The regulation of gene expression required for C_4 photosynthesis. *Annu. Rev. Plant Biol.* 61:181–207
81. Hibberd JM, Quick WP. 2002. Characteristics of C_4 photosynthesis in stems and petioles of C_3 plants. *Nature* 415:451–54
82. Huang P, Studer AJ, Schnable JC, Kellogg EA, Brutnell TP. 2017. Cross species selection scans identify components of C_4 photosynthesis in the grasses. *J. Exp. Bot.* 68(2):127–35
83. Hughes T, Sedelnikova OV, Wu H, Becraft P, Langdale JA. 2019. Redundant *SCARECROW* genes pattern distinct cell layers in roots and leaves of maize. *Development* 146:dev177543

84. Hylton CM, Rawsthorne S, Smith AM, Jones DA, Woolhouse HW. 1988. Glycine decarboxylase is confined to the bundle-sheath cells of leaves of C_3–C_4 intermediate species. *Planta* 175(4):452–59
85. Jacobs B, Engelmann S, Westhoff P, Gowik U. 2008. Evolution of C_4 phosphoenolpyruvate carboxylase in *Flaveria*: determinants for high tolerance towards the inhibitor L-malate. *Plant Cell Environ*. 31(6):793–803
86. John CR, Smith-Unna RD, Woodfield H, Covshoff S, Hibberd JM. 2014. Evolutionary convergence of cell-specific gene expression in independent lineages of C_4 grasses. *Plant Physiol*. 165(1):62–75
87. Kajala K, Brown NJ, Williams BP, Borrill P, Taylor LE, Hibberd JM. 2012. Multiple Arabidopsis genes primed for recruitment into C_4 photosynthesis. *Plant J*. 69(1):47–56
88. Kanai R, Edwards GE. 1999. The biochemistry of C_4 photosynthesis. In *C4 Plant Biology*, ed. RF Sage, RK Monson, pp. 49–87. London: Academic
89. Kano-Murakami Y, Suzuki I, Sugiyama T, Matsuoka M. 1991. Sequence-specific interactions of a maize factor with a GC-rich repeat in the phosphoenolpyruvate carboxylase gene. *Mol. Genet. Genom.* 225:203–8
90. Kausch AP, Owen TP, Zachwieja SJ, Flynn AR, Sheen J. 2001. Mesophyll-specific, light and metabolic regulation of the C_4 PPCZm1 promoter in transgenic maize. *Plant Mol. Biol.* 45(1):1–15
91. Khoshravesh R, Akhani H, Sage TL, Nordenstam B, Sage RF. 2012. Phylogeny and photosynthetic pathway distribution in *Anticharis* Endl. (Scrophulariaceae). *J. Exp. Bot.* 63(15):5645–58
92. Khoshravesh R, Stinson CR, Stata M, Busch FA, Sage RF, et al. 2016. C_3–C_4 intermediacy in grasses: organelle enrichment and distribution, glycine decarboxylase expression, and the rise of C_2 photosynthesis. *J. Exp. Bot.* 67(10):3065–78
93. Kirschner S, Woodfield H, Prusko K, Koczor M, Gowik U, et al. 2018. Expression of *SULTR2;2*, encoding a low-affinity sulphur transporter, in the Arabidopsis bundle sheath and vein cells is mediated by a positive regulator. *J. Exp. Bot.* 69(20):4897–906
94. Kleczkowski LA, Randall DD. 1986. Thiol-dependent regulation of glycerate metabolism in leaf extracts: the role of glycerate kinase in C_4 plants. *Plant Physiol*. 81(2):656–62
95. Kopriva S, Jones A, Koprivova A, Suter M, von Ballmoos P, et al. 2001. Influence of chilling stress on the intercellular distribution of assimilatory sulfate reduction and thiols in *Zea mays*. *Plant Biol*. 3(1):24–31
96. Kromdijk J, Griffiths H, Schepers HE. 2010. Can the progressive increase of C_4 bundle sheath leakiness at low PFD be explained by incomplete suppression of photorespiration? *Plant Cell Environ*. 33(11):1935–48
97. Kubásek J, Urban O, Šantrůček J. 2013. C_4 plants use fluctuating light less efficiently than do C_3 plants: a study of growth, photosynthesis and carbon isotope discrimination. *Physiol. Plant* 149(4):528–39
98. Kubicki A, Funk E, Westhoff P, Steinmüller K. 1996. Differential expression of plastome-encoded *ndh* genes in mesophyll and bundle-sheath chloroplasts of the C_4 plant *Sorghum bicolor* indicates that the complex I-homologous NAD(P)H-plastoquinone oxidoreductase is involved in cyclic electron transport. *Planta* 199:276–81
99. Külahoglu C, Denton AK, Sommer M, Maß J, Schliesky S, et al. 2014. Comparative transcriptome atlases reveal altered gene expression modules between two Cleomaceae C_3 and C_4 plant species. *Plant Cell* 26(8):3243–60
100. Kumar RA, Oldenburg DJ, Bendich AJ. 2015. Molecular integrity of chloroplast DNA and mitochondrial DNA in mesophyll and bundle sheath cells of maize. *Planta* 241(5):1221–30
101. Kümpers BMC, Burgess SJ, Reyna-Llorens I, Smith-Unna R, Boursnell C, Hibberd JM. 2017. Shared characteristics underpinning C_4 leaf maturation derived from analysis of multiple C_3 and C_4 species of *Flaveria*. *J. Exp. Bot*. 68(2):177–89
102. Lai LB, Wang L, Nelson TM. 2002. Distinct but conserved functions for two chloroplastic NADP-malic enzyme isoforms in C_3 and C_4 *Flaveria* species. *Plant Physiol*. 128(1):125–39
103. Langdale JA. 2011. C_4 cycles: past, present, and future research on C_4 photosynthesis. *Plant Cell* 23(11):3879–92
104. Langdale JA, Kidner CA. 1994. Bundle sheath defective, a mutation that disrupts cellular differentiation in maize leaves. *Development* 120(3):673–81

105. Langdale JA, Taylor WC, Nelson T. 1991. Cell-specific accumulation of maize phosphoenolpyruvate carboxylase is correlated with demethylation at a specific site >3 kb upstream of the gene. *Mol. Gen. Genet.* 225(1):49–55
106. Leegood RC, von Caemmerer S. 1989. Some relationships between contents of photosynthetic intermediates and the rate of photosynthetic carbon assimilation in leaves of *Zea mays* L. *Planta* 178:258–66
107. Leegood RC, Walker RP. 2003. Regulation and roles of phospho*enol*pyruvate carboxykinase in plants. *Arch. Biochem. Biophys.* 414(2):204–10
108. Levey M, Timm S, Mettler-Altmann T, Borghi GL, Koczor M, et al. 2019. Efficient 2-phosphoglycolate degradation is required to maintain carbon assimilation and allocation in the C_4 plant *Flaveria bidentis*. *J. Exp. Bot.* 70(2):575–87
109. Li P, Ponnala L, Gandotra N, Wang L, Si Y, et al. 2010. The developmental dynamics of the maize leaf transcriptome. *Nat. Genet.* 42(12):1060–67
110. Long SP. 1999. Environmental responses. In *C_4 Plant Biology*, ed. RF Sage, RK Monson, pp. 215–49. London: Academic
111. Ludwig M. 2012. Carbonic anhydrase and the molecular evolution of C_4 photosynthesis. *Plant Cell Environ.* 35(1):22–37
112. Lundgren MR, Christin P-A, Escobar EG, Ripley BS, Besnard G, et al. 2016. Evolutionary implications of C_3–C_4 intermediates in the grass *Alloteropsis semialata*. *Plant Cell Environ.* 39(9):1874–85
113. Lundgren MR, Dunning LT, Olofsson JK, Moreno-Villena JJ, Bouvier JW, et al. 2019. C_4 anatomy can evolve via a single developmental change. *Ecol. Lett.* 22(2):302–12
114. Majeran W, Cai Y, Sun Q, van Wijk KJ. 2005. Functional differentiation of bundle sheath and mesophyll maize chloroplasts determined by comparative proteomics. *Plant Cell* 17(11):3111–40
115. Mallmann J, Heckmann D, Bräutigam A, Lercher MJ, Weber APM, et al. 2014. The role of photorespiration during the evolution of C_4 photosynthesis in the genus *Flaveria*. *eLife* 3:e02478
116. Marshall JS, Stubbs JD, Chitty JA, Surin B, Taylor WC. 1997. Expression of the C_4 *Me1* gene from *Flaveria bidentis* requires an interaction between 5′ and 3′ sequences. *Plant Cell* 9(9):1515–25
117. Matsuoka M, Kyozuka J, Shimamoto K, Kano-Murakami Y. 1994. The promoters of two carboxylases in a C_4 plant (maize) direct cell-specific, light-regulated expression in a C_3 plant (rice). *Plant J.* 6(3):311–19
118. Matsuoka M, Numazawa T. 1991. *CIS*-acting elements in the pyruvate, orthophosphate dikinase gene from maize. *Mol. Gen. Genet.* 228(1–2):143–52
119. Matsuoka M, Sanada Y. 1991. Expression of photosynthetic genes from the C_4 plant, maize, in tobacco. *Mol. Gen. Genet.* 225(3):411–19
120. Mayfield SP, Taylor WC. 1984. The appearance of photosynthetic proteins in developing maize leaves. *Planta* 161:481–86
121. McKown AD, Moncalvo J-M, Dengler NG. 2005. Phylogeny of *Flaveria* (Asteraceae) and inference of C_4 photosynthesis evolution. *Am. J. Bot.* 92(11):1911–28
122. Meister M, Agostino A, Hatch MD. 1996. The roles of malate and aspartate in C_4 photosynthetic metabolism of *Flaveria bidentis* (L.). *Planta* 199:262–69
123. Michelet L, Zaffagnini M, Morisse S, Sparla F, Pérez-Pérez ME, et al. 2013. Redox regulation of the Calvin-Benson cycle: something old, something new. *Front. Plant Sci.* 4:470
124. Miyake H. 2016. Starch accumulation in the bundle sheaths of C_3 plants: a possible pre-condition for C_4 photosynthesis. *Plant Cell Physiol.* 57(5):890–96
125. Monson RK, Rawsthorne S. 2000. CO_2 assimilation in C_3-C_4 intermediate plants. In *Photosynthesis: Physiology and Metabolism*, ed. RC Leegood, TD Sharkey, S von Caemmerer, pp. 533–50. Dordrecht, Neth.: Springer
126. Moore R, Black CJ. 1979. Nitrogen assimilation pathways in leaf mesophyll and bundle sheath cells of C_4 photosynthesis plants formulated from comparative studies with *Digitaria sanguinalis* (L.) Scop. *Plant Physiol.* 64:309–13
127. Moreno-Villena JJ, Dunning LT, Osborne CP, Christin P-A. 2018. Highly expressed genes are preferentially co-opted for C_4 photosynthesis. *Mol. Biol. Evol.* 35(1):94–106
128. Muhaidat R, Sage TL, Frohlich MW, Dengler NG, Sage RF. 2011. Characterization of C_3–C_4 intermediate species in the genus *Heliotropium* L. (Boraginaceae): anatomy, ultrastructure and enzyme activity. *Plant Cell Environ.* 34(10):1723–36

129. Munekage YN, Taniguchi YY. 2016. Promotion of cyclic electron transport around photosystem I with the development of C_4 photosynthesis. *Plant Cell Physiol*. 57(5):897–903
130. Nakamura H, Muramatsu M, Hakata M, Ueno O, Nagamura Y, et al. 2009. Ectopic overexpression of the transcription factor *OsGLK1* induces chloroplast development in non-green rice cells. *Plant Cell Physiol*. 50(11):1933–49
131. Nikkanen L, Rintamäki E. 2019. Chloroplast thioredoxin systems dynamically regulate photosynthesis in plants. *Biochem. J.* 476(7):1159–72
132. Nikkanen L, Toivola J, Diaz MG, Rintamäki E. 2017. Chloroplast thioredoxin systems: prospects for improving photosynthesis. *Philos. Trans. R. Soc. B* 372(1730):20160474
133. Niklaus M, Kelly S. 2019. The molecular evolution of C_4 photosynthesis: opportunities for understanding and improving the world's most productive plants. *J. Exp. Bot.* 70(3):859–69
134. Nomura M, Higuchi T, Ishida Y, Ohta S, Komari T, et al. 2005. Differential expression pattern of C_4 bundle sheath expression genes in rice, a C_3 plant. *Plant Cell Physiol*. 46(5):754–61
135. Nomura M, Sentoku N, Nishimura A, Lin J-H, Honda C, et al. 2000. The evolution of C_4 plants: acquisition of *cis*-regulatory sequences in the promoter of C_4-type pyruvate, orthophosphate dikinase gene. *Plant J.* 22(3):211–21
136. Ohnishi J, Flügge UI, Heldt HW. 1989. Phosphate translocator of mesophyll and bundle sheath chloroplasts of a C_4 plant, *Panicum miliaceum* L.: identification and kinetic characterization. *Plant Physiol*. 91:1507–11
137. Patel M, Corey AC, Yin L, Ali S, Taylor WC, Berry JO. 2004. Untranslated regions from C_4 amaranth *AhRbc*S1 mRNAs confer translational enhancement and preferential bundle sheath cell expression in transgenic C_4 *Flaveria bidentis*. 136(3):3550–61
138. Patel M, Siegel AJ, Berry JO. 2006. Untranslated regions of *FbRbc*S1 mRNA mediate bundle sheath cell-specific gene expression in leaves of a C_4 plant. *J. Biol. Chem.* 281(35):25485–91
139. Paulus JK, Schlieper D, Groth G. 2013. Greater efficiency of photosynthetic carbon fixation due to single amino-acid substitution. *Nat. Commun.* 4:1518
140. Perduns R, Horst-Niessen I, Peterhansel C. 2015. Photosynthetic genes and genes associated with the C_4 trait in maize are characterized by a unique class of highly regulated histone acetylation peaks on upstream promoters. *Plant Physiol*. 168(4):1378–88
141. Pick TR, Brautigam A, Schluter U, Denton AK, Colmsee C, et al. 2011. Systems analysis of a maize leaf developmental gradient redefines the current C_4 model and provides candidates for regulation. *Plant Cell* 23(12):4208–20
142. Pinto H, Powell JR, Sharwood RE, Tissue DT, Ghannoum O. 2016. Variations in nitrogen use efficiency reflect the biochemical subtype while variations in water use efficiency reflect the evolutionary lineage of C_4 grasses at inter-glacial CO_2. *Plant Cell Environ*. 39(3):514–26
143. Purcell M, Mabrouk YM, Bogorad L. 1995. Red/far-red and blue light-responsive regions of maize *rbcS*-m3 are active in bundle sheath and mesophyll cells, respectively. *PNAS* 92(25):11504–8
144. Rao X, Lu N, Li G, Nakashima J, Tang Y, Dixon RA. 2016. Comparative cell-specific transcriptomics reveals differentiation of C_4 photosynthesis pathways in switchgrass and other C_4 lineages. *J. Exp. Bot.* 67(6):1649–62
145. Rawsthorne S, Hylton CM, Smith AM, Woolhouse HW. 1988. Distribution of photorespiratory enzymes between bundle-sheath and mesophyll cells in leaves of the C_3–C_4 intermediate species *Moricandia arvensis* (L.) DC. *Planta* 176:527–32
146. Rawsthorne S, Hylton CM, Smith AM, Woolhouse HW. 1988. Photorespiratory metabolism and immunogold localization of photorespiratory enzymes in leaves of C_3 and C_3-C_4 intermediate species of *Moricandia*. *Planta* 173:298–308
147. Reeves G, Grangé-Guermente MJ, Hibberd JM. 2017. Regulatory gateways for cell-specific gene expression in C_4 leaves with Kranz anatomy. *J. Exp. Bot.* 68(2):107–16
148. Reyna-Llorens I, Burgess SJ, Reeves G, Singh P, Stevenson SR, et al. 2018. Ancient duons may underpin spatial patterning of gene expression in C_4 leaves. *PNAS* 115(8):1931–36
149. Reyna-Llorens I, Hibberd JM. 2017. Recruitment of pre-existing networks during the evolution of C_4 photosynthesis. *Philos. Trans. R. Soc. B* 372(1730):20160386

150. Rosche E, Chitty J, Westhoff P, Taylor WC. 1998. Analysis of promoter activity for the gene encoding pyruvate orthophosphate dikinase in stably transformed C_4 *Flaveria* species. *Plant Physiol.* 117:821–29
151. Rosnow JJ, Edwards GE, Roalson EH. 2014. Positive selection of Kranz and non-Kranz C_4 phosphoenolpyruvate carboxylase amino acids in Suaedoideae (Chenopodiaceae). *J. Exp. Bot.* 65(13):3595–607
152. Roth R, Hall LN, Brutnell TP, Langdale JA. 1996. bundle sheath defective2, a mutation that disrupts the coordinated development of bundle sheath and mesophyll cells in the maize leaf. *Plant Cell* 8:915–27
153. Sage RF. 2004. The evolution of C_4 photosynthesis. *New Phytol.* 161(2):341–70
154. Sage RF. 2016. A portrait of the C_4 photosynthetic family on the 50th anniversary of its discovery: species number, evolutionary lineages, and Hall of Fame. *J. Exp. Bot.* 67(14):4039–56
155. Sage RF, Christin P-A, Edwards EJ. 2011. The C_4 plant lineages of planet Earth. *J. Exp. Bot.* 62(9):3155–69
156. Sage RF, Sage TL, Kocacinar F. 2012. Photorespiration and the evolution of C_4 photosynthesis. *Annu. Rev. Plant Biol.* 63:19–47
157. Sage TL, Sage RF, Vogan PJ, Rahman B, Johnson DC, et al. 2011. The occurrence of C_2 photosynthesis in *Euphorbia* subgenus *Chamaesyce* (Euphorbiaceae). *J. Exp. Bot.* 62(9):3183–95
158. Schäffner AR, Sheen J. 1991. Maize *rbcS* promoter activity depends on sequence elements not found in dicot *rbcS* promoters. *Plant Cell* 3:997–1012
159. Schlüter U, Bräutigam A, Droz JM, Schwender J, Weber APM. 2019. The role of alanine and aspartate aminotransferases in C_4 photosynthesis. *Plant Biol.* 21(S1):64–76
160. Schlüter U, Bräutigam A, Gowik U, Melzer M, Christin P-A, et al. 2017. Photosynthesis in C_3–C_4 intermediate *Moricandia* species. *J. Exp. Bot.* 68(2):191–206
161. Schlüter U, Denton AK, Bräutigam A. 2016. Understanding metabolite transport and metabolism in C_4 plants through RNA-seq. *Curr. Opin. Plant Biol.* 31:83–90
162. Schulze S, Mallmann J, Burscheidt J, Koczor M, Streubel M, et al. 2013. Evolution of C_4 photosynthesis in the genus *Flaveria*: establishment of a photorespiratory CO_2 pump. *Plant Cell* 25(7):2522–35
163. Schüssler C, Freitag H, Koteyeva N, Schmidt D, Edwards G, et al. 2017. Molecular phylogeny and forms of photosynthesis in tribe Salsoleae (Chenopodiaceae). *J. Exp. Bot.* 68(2):207–23
164. Sedelnikova OV, Hughes TE, Langdale JA. 2018. Understanding the genetic basis of C_4 Kranz anatomy with a view to engineering C_3 crops. *Annu. Rev. Genet.* 52:249–70
165. Sharwood RE, Ghannoum O, Whitney SM. 2016. Prospects for improving CO_2 fixation in C_3-crops through understanding C_4-Rubisco biogenesis and catalytic diversity. *Curr. Opin. Plant Biol.* 31:135–42
166. Sheen J. 1991. Molecular mechanisms underlying the differential expression of maize pyruvate, orthophosphate dikinase genes. *Plant Cell* 3:225–45
167. Shen Z, Dong XM, Gao ZF, Chao Q, Wang BC. 2017. Phylogenic and phosphorylation regulation difference of phosphoenolpyruvate carboxykinase of C_3 and C_4 plants. *J. Plant Physiol.* 213:16–22
168. Slewinski TL, Anderson AA, Zhang C, Turgeon R. 2012. *Scarecrow* plays a role in establishing Kranz anatomy in maize leaves. *Plant Cell Physiol.* 53(12):2030–37
169. Sommer M, Bräutigam A, Weber APM. 2012. The dicotyledonous NAD malic enzyme C_4 plant Cleome gynandra displays age-dependent plasticity of C_4 decarboxylation biochemistry. *Plant Biol.* 14(4):621–29
170. Sonawane BV, Sharwood RE, Whitney S, Ghannoum O. 2018. Shade compromises the photosynthetic efficiency of NADP-ME less than that of PEP-CK and NAD-ME C_4 grasses. *J. Exp. Bot.* 69(12):3053–68
171. Stitt M, Heldt HW. 1985. Generation and maintenance of concentration gradients between the mesophyll and bundle sheath in maize leaves. *Biochim. Biophys. Acta* 808(3):400–14
172. Studer AJ, Gandin A, Kolbe AR, Wang L, Cousins AB, Brutnell TP. 2014. A limited role for carbonic anhydrase in C_4 photosynthesis as revealed by a *ca1ca2* double mutant in maize. *Plant Physiol.* 165(2):608–17
173. Takabayashi A, Kishine M, Asada K, Endo T, Sato F. 2005. Differential use of two cyclic electron flows around photosystem I for driving CO_2-concentration mechanism in C_4 photosynthesis. *PNAS* 102(46):16898–903
174. Taniguchi M, Izawa K, Ku MSB, Lin J-H, Saito H, et al. 2000. Binding of cell type-specific nuclear proteins to the 5′-flanking region of maize C_4 phospho*enol*pyruvate carboxylase gene confers its differential transcription in mesophyll cells. *Plant Mol. Biol.* 44:543–57

175. Tanz SK, Tetu SG, Vella NGF, Ludwig M. 2009. Loss of the transit peptide and an increase in gene expression of an ancestral chloroplastic carbonic anhydrase were instrumental in the evolution of the cytosolic C_4 carbonic anhydrase in *Flaveria*. *Plant Physiol.* 150(3):1515–29
176. Tausta LS, Li P, Si Y, Gandotra N, Liu P, et al. 2014. Developmental dynamics of Kranz cell transcriptional specificity in maize leaf reveals early onset of C_4-related processes. *J. Exp. Bot.* 65(13):3543–55
177. Tipping C, Murray DR. 1999. Effects of elevated atmospheric CO_2 concentration on leaf anatomy and morphology in *Panicum* species representing different photosynthetic modes. *Int. J. Plant Sci.* 160(6):1363–73
178. Turkan I, Uzilday B, Dietz KJ, Bräutigam A, Ozgur R. 2018. Reactive oxygen species and redox regulation in mesophyll and bundle sheath cells of C_4 plants. *J. Exp. Bot.* 69(14):3321–31
179. Ueno O. 2011. Structural and biochemical characterization of the C_3-C_4 intermediate *Brassica gravinae* and relatives, with particular reference to cellular distribution of Rubisco. *J. Exp. Bot.* 62(15):5347–55
180. Ueno O, Wada Y, Wakai M, Bang SW. 2006. Evidence from photosynthetic characteristics for the hybrid origin of *Diplotaxis muralis* from a C_3-C_4 intermediate and a C_3 species. *Plant Biol.* 8(2):253–59
181. Usuda H. 1987. Changes in levels of intermediates of the C_4 cycle and reductive pentose phosphate pathway under various light intensities in maize leaves. *Plant Physiol.* 83:29–32
182. Usuda H, Edwards GE. 1980. Localization of glycerate kinase and some enzymes for sucrose synthesis in C_3 and C_4 plants. *Plant Physiol.* 65:1017–22
183. Viret J-F, Mabrouk YM, Bogorad L. 1994. Transcriptional photoregulation of cell-type-preferred expression of maize *rbcS*-m3: 3′ and 5′ sequences are involved. *PNAS* 91:8577–81
184. Vogan PJ, Frohlich MW, Sage RF. 2007. The functional significance of C_3–C_4 intermediate traits in *Heliotropium* L. (Boraginaceae): gas exchange perspectives. *Plant Cell Environ.* 30(10):1337–45
185. von Caemmerer S, Quinn V, Hancock NC, Price GD, Furbank RT, Ludwig M. 2004. Carbonic anhydrase and C_4 photosynthesis: atransgenic analysis. *Plant Cell Environ.* 27(6):697–703
186. Voznesenskaya EV, Franceschi VR, Kiirats O, Artyusheva EG, Freitag H, Edwards GE. 2002. Proof of C_4 photosynthesis without Kranz anatomy in *Bienertia cycloptera* (Chenopodiaceae). *Plant J.* 31(5):649–62
187. Voznesenskaya EV, Koteyeva NK, Akhani H, Roalson EH, Edwards GE. 2013. Structural and physiological analyses in Salsoleae (Chenopodiaceae) indicate multiple transitions among C_3, intermediate, and C_4 photosynthesis. *J. Exp. Bot.* 64(12):3583–604
188. Voznesenskaya EV, Koteyeva NK, Edwards GE, Ocampo G. 2010. Revealing diversity in structural and biochemical forms of C_4 photosynthesis and a C_3–C_4 intermediate in genus *Portulaca* L. (Portulacaceae). *J. Exp. Bot.* 61(13):3647–62
189. Wang D, Portis AR, Moose SP, Long SP. 2008. Cool C_4 photosynthesis: Pyruvate P_i dikinase expression and activity corresponds to the exceptional cold tolerance of carbon assimilation in *Miscanthus* × *giganteus*. *Plant Physiol.* 148(1):557–67
190. Wang L, Czedik-Eysenberg A, Mertz RA, Si Y, Tohge T, et al. 2014. Comparative analyses of C_4 and C_3 photosynthesis in developing leaves of maize and rice. *Nat. Biotechnol.* 32(11):1158–65
191. Wang P, Karki S, Biswal AK, Lin H-C, Dionora MJ, et al. 2017. Candidate regulators of early leaf development in maize perturb hormone signalling and secondary cell wall formation when constitutively expressed in rice. *Sci. Rep.* 7(1):4535
192. Wang P, Kelly S, Fouracre JP, Langdale JA. 2013. Genome-wide transcript analysis of early maize leaf development reveals gene cohorts associated with the differentiation of C_4 Kranz anatomy. *Plant J.* 75(4):656–70
193. Wang P, Khoshravesh R, Karki S, Tapia R, Balahadia CP, et al. 2017. Re-creation of a key step in the evolutionary switch from C_3 to C_4 leaf anatomy. *Curr. Biol.* 27(21):3278–87.e6
194. Watcharamongkol T, Christin PA, Osborne CP. 2018. C_4 photosynthesis evolved in warm climates but promoted migration to cooler ones. *Ecol. Lett.* 21(3):376–83
195. Weckopp SC, Kopriva S. 2015. Are changes in sulfate assimilation pathway needed for evolution of C_4 photosynthesis? *Front. Plant Sci.* 5:773
196. Westhoff P, Gowik U. 2004. Evolution of C_4 phosphoenolpyruvate carboxylase. Genes and proteins: a case study with the genus *Flaveria*. *Ann. Bot.* 93(1):13–23

197. Williams BP, Burgess SJ, Reyna-Llorens I, Knerova J, Aubry S, et al. 2016. An untranslated *cis*-element regulates the accumulation of multiple C_4 enzymes in *Gynandropsis gynandra* mesophyll cells. *Plant Cell* 28(2):454–65
198. Williams BP, Johnston IG, Covshoff S, Hibberd JM. 2013. Phenotypic landscape inference reveals multiple evolutionary paths to C_4 photosynthesis. *eLife* 2:e00961
199. Wiludda C, Schulze S, Gowik U, Engelmann S, Koczor M, et al. 2012. Regulation of the photorespiratory *GLDPA* gene in C_4 *Flaveria*: an intricate interplay of transcriptional and posttranscriptional processes. *Plant Cell* 24(1):137–51
200. Windhövel A, Hein I, Dabrowa R, Stockhaus J. 2001. Characterization of a novel class of plant homeodomain proteins that bind to the C_4 phosphoenolpyruvate carboxylase gene of *Flaveria trinervia*. *Plant Mol. Biol.* 45:201–14
201. Xu T, Purcell M, Zucchi P, Helentjaris T, Bogorad L. 2002. TRM1, a YY1-like suppressor of *rbcS-m3* expression in maize mesophyll cells. *PNAS* 98(5):2295–300
202. Yanagisawa S. 2000. Dof1 and Dof2 transcription factors are associated with expression of multiple genes involved in carbon metabolism in maize. *Plant J.* 21(3):281–88
203. Yerramsetty P, Stata M, Siford R, Sage TL, Sage RF, et al. 2016. Evolution of RLSB, a nuclear-encoded S1 domain RNA binding protein associated with post-transcriptional regulation of plastid-encoded *rbc*L mRNA in vascular plants. *BMC Evol. Biol.* 16(1):141
204. Yu C-P, Chen SC-C, Chang Y-M, Liu W-Y, Lin H-H, et al. 2015. Transcriptome dynamics of developing maize leaves and genomewide prediction of *cis* elements and their cognate transcription factors. *PNAS* 112(19):E2477–86
205. Zelitch I, Schultes NP, Peterson RB, Brown P, Brutnell TP. 2009. High glycolate oxidase activity is required for survival of maize in normal air. *Plant Physiol.* 149(1):195–204
206. Zhang YG, Pagani M, Liu Z, Bohaty SM, Deconto R. 2013. A 40-million-year history of atmospheric CO_2. *Philos. Trans. R. Soc. A* 371:20130096
207. Zhou H, Helliker BR, Huber M, Dicks A, Akçay E. 2018. C_4 photosynthesis and climate through the lens of optimality. *PNAS* 115(47):12057–62